J Comput Neurosci
DOI 10.1007/s10827-008-0084-8

Modeling the role of lateral membrane diffusion in AMPA receptor trafficking along a spiny dendrite

B. A. Earnshaw · P. C. Bressloff

Received: 1 November 2007 / Revised: 2 January 2008 / Accepted: 1 February 2008

Abstract AMPA receptor trafficking in dendritic spines is emerging as a major postsynaptic mechanism for the expression of plasticity at glutamatergic synapses. AMPA receptors within a spine are in a continuous state of flux, being exchanged with local intracellular pools via exo/endocytosis and with the surrounding dendrite via lateral membrane diffusion. This suggests that one cannot treat a single spine in isolation. Here we present a model of AMPA receptor trafficking between multiple dendritic spines distributed along the surface of a dendrite. Receptors undergo lateral diffusion within the dendritic membrane, with each spine acting as a spatially localized trap where receptors can bind to scaffolding proteins or be internalized through endocytosis. Exocytosis of receptors occurs either at the soma or at sites local to dendritic spines via constitutive recycling from intracellular pools. We derive a reaction–diffusion equation for receptor trafficking that takes into account these various processes. Solutions of this equation allow us to calculate the distribution of synaptic receptor numbers across the population of spines, and hence determine how lateral diffusion contributes to the strength of a synapse. A number of specific results follow from our modeling and analysis. (1) Lateral membrane diffusion alone is insufficient as a mechanism for delivering AMPA receptors from the soma to distal dendrites. (2) A source of surface receptors at the soma tends to generate an exponential-like distribution of receptors along the dendrite, which has implications for synaptic democracy. (3) Diffusion mediates a heterosynaptic interaction between spines so that local changes in the constitutive recycling of AMPA receptors induce nonlocal changes in synaptic strength. On the other hand, structural changes in a spine following long term potentiation or depression have a purely local effect on synaptic strength. (4) A global change in the rates of AMPA receptor exo/endocytosis is unlikely to be the sole mechanism for homeostatic synaptic scaling. (5) The dynamics of AMPA receptor trafficking occurs on multiple timescales and varies according to spatial location along the dendrite. Understanding such dynamics is important when interpreting data from inactivation experiments that are used to infer the rate of relaxation to steady-state.

Keywords AMPA receptor · Receptor tracking · Membrane diffusion · Dendritic spine · Synaptic plasticity · Cable equation

Action Editor: John Rinzel

B. A. Earnshaw · P. C. Bressloff (✉)
Department of Mathematics, University of Utah,
Salt Lake City, UT 84112, USA
e-mail: bressloff@math.utah.edu

1 Introduction

There is a growing body of experimental evidence suggesting that the trafficking of α-amino-3-hydroxy-5-methyl-4-isoxazole-propionic acid (AMPA) receptors, which mediate the majority of fast excitatory synaptic transmission in the central nervous system, contributes to activity-dependent, long-lasting changes in synaptic strength (Malinow and Malenka 2002; Song and Huganir 2002; Sheng and Kim 2002; Bredt and Nicoll 2003; Collingridge et al. 2004; Derkach et al. 2007). AMPA receptors cluster at synapses through

interactions with scaffolding proteins and cytoskeletal elements within the postsynaptic density (PSD), which is the protein-rich domain in the postsynaptic membrane of a dendritic spine that is directly apposed to the presynaptic active zone. Given that hundreds or thousands of synapses and their associated spines are distributed along the length of a dendrite, it follows that neurons must traffic receptors and other postsynaptic proteins over long distances (several 100 μm) from the soma or cell body where they are synthesized to distal regions of a dendrite. This can occur by two distinct mechanisms: either by lateral diffusion within the plasma membrane (Choquet and Trillier 2003; Triller and Choquet 2003, 2005; Kennedy and Ehlers 2006; Chen et al. 2007) or by motor-driven microtubular transport to local intracellular pools, followed by direct insertion into the surface of the spine via exocytosis (Kim and Lisman 2001; Setou et al. 2002). A variety of optical, biochemical and electrophysiological experiments find that synaptic AMPA receptors constitutively recycle between the surface and local intracellular pools in 10–30 min (Luscher et al. 1999; Ehlers 2000; Lin et al. 2000; Passafaro et al. 2001), suggesting a model wherein local intracellular pools are the primary source of synaptic AMPA receptors, and exchange with these pools combined with local surface diffusion is the major mode of trafficking. In contrast, recent work by Adesnik et al. (2005) based on the photoinactivation of surface receptors finds synaptic recycling requires up to 16 hr whereas somatic recycling is still fast, implicating reserves of surface AMPA receptors as the primary source of synaptic AMPA receptors and lateral diffusion from the soma as the major trafficking mode.

In this paper we investigate the role of membrane diffusion in the local and non-local trafficking of AMPA receptors by extending our recent model of receptor trafficking at a single dendritic spine (Earnshaw and Bressloff 2006). The model spine consists of two compartments: the postsynaptic density (PSD) of the spine head, and the extrasynaptic membrane (ESM) of the remaining spine head. Diffusion of free receptors within each compartment is assumed to be sufficiently fast so that the corresponding receptor concentrations can be treated as spatially uniform. AMPA receptors move between the two compartments and between the spine and surrounding dendrite, bind to scaffolding proteins within the PSD and exchange with local intracellular pools via exo/endocytosis. Assuming that synaptic strength is determined by the number of synaptic AMPA receptors, we have shown how our single-spine model reproduces a variety of experimental data, including changes in synaptic strength consistent with those found during *N*-methyl-D-aspartate (NMDA) receptor-mediated long term potentiation (LTP; Bliss and Lomo 1973) and long-term depression (LTD; Dudek and Bear 1992, 1993). One of the simplifications of our single-spine model was to take the dendritic receptor concentration in the vicinity of the spine to be fixed at some background concentration. Here we extend our single-spine model to a continuous population of spines distributed along a one-dimensional dendritic cable, with receptors trafficking between spines and other neuronal compartments such as the soma via membrane diffusion within the dendrite (see Section 2). The multi-spine model allows us to determine the background dendritic receptor concentration *ab initio* by solving an associated diffusion equation that is coupled to the internal spine kinetics. This solution can then be used to calculate the distribution of synaptic receptors across the population of spines and hence to explore the role of lateral diffusion in AMPA receptor trafficking.

First, we determine the steady-state distribution of synaptic AMPA receptors for a population of identical spines distributed uniformly along the dendrite by solving an effective "cable" equation for AMPA receptor trafficking (Section 3.1). We show that if there is a source of surface receptors at the soma then the distribution of synaptic receptors decays exponentially away from the soma at a rate determined by the space constant of the associated cable equation; such an exponential distribution has also been observed experimentally (Piccini and Malinow 2002). The space constant depends on the spine density, the surface diffusivity, the hopping rate between dendrite and spines, as well as various parameters associated with constitutive recycling. The exponential-like distribution of receptors suggests that in order to supply distal synapses with receptors it is necessary to supplement lateral diffusion of surface receptors from the soma with an additional delivery mechanism such as motor-assisted transport combined with constitutive recycling. Moreover, some form of inhomogeneity in spine properties is needed in order to maintain synaptic democracy (Hausser 2001; Rumsey and Abbott 2006). Next we consider how lateral diffusion mediates heterosynaptic interactions between spines, and show how the spatial scale of heterosynaptic interactions depends on the space constant of the associated cable equation (Section 3.2). In particular, we establish that the various spine properties can be classified according to their degree of local versus non-local influence on synaptic receptor numbers. For example, a change in the number and/or affinity of scaffolding proteins within the PSD of a spine has a purely local effect, whereas a variation in the rates of receptor exo/endocytosis has both a local as well as a non-local effect. Since LTP and LTD are

thought to involve local changes in the structure of a spine, we thus conclude that surface diffusion of AMPA receptors is unlikely on its own to mediate a form of heterosynaptic plasticity. We end our steady-state analysis by investigating to what extent regulating the rates of constitutive recycling provides an expression mechanism for homeostatic synaptic scaling (Section 3.3). The latter refers to the experimental finding that a chronic increase/decrease in average cortical activity induces a global and multiplicative scaling of synaptic AMPA receptor-mediated miniature excitatory postsynaptic currents (mEPSCs) in the opposite direction, thus compensating for the slow cumulative changes in activity (Turrigiano et al. 1998; O'Brien et al. 1998; Turrigiano and Nelson 2004; Davis 2006). Given that synaptic scaling appears to be associated with a corresponding increase or decrease in the number of synaptic AMPA receptors, it has been hypothesized that synaptic scaling involves a global change in the rate of AMPA receptor exocytosis and/or endocytosis (Turrigiano and Nelson 2004). We show that this is unlikely to be the sole mechanism for synaptic scaling and that this is a consequence of spatial variations in the dendritic receptor concentration and nonlinearities arising from the kinetics of receptors binding to scaffolding proteins within the PSD.

In the final part of the paper (Section 4) we address the issue of fast versus slow constitutive recycling by simulating the photoinactivation experiments of Adesnik et al. (2005). We proceed by numerically solving the full time-dependent reaction–diffusion model given an initial condition obtained by taking the steady-state solution and instantaneously inactivating all surface receptors. We then track the inactive receptors separately from the active receptors that were in an intracellular pool at time $t = 0$ or are synthesized thereafter. Inactive receptors traffick in the same way as their active counterparts, except that once an inactive receptor is endocytosed it is sorted for degradation and never reinserted into the neuronal membrane. We find that a number of distinct factors contribute to the recovery process including the rate at which new receptors are inserted into the PSD from intracellular pools, the rate of refilling of the intracellular pools, and the rate at which receptors unbind from scaffolding proteins. We thus establish that recovery following photoinactivation occurs on multiple timescales and varies according to spatial location along the dendrite. Hence, there may not be a clear distinction between fast and slow constitutive recycling, as currently assumed in the experimental literature (Chen et al. 2007).

We note that there are a number of other biophysical models of AMPA receptor trafficking and its role in synaptic plasticity (Castellani et al. 2001; Shouval et al. 2002a, b; Hayer and Bhalla 2005; Shouval 2005; Holmes and Grover 2006; Zhabotinsky et al. 2006; Holcman and Triller 2006). These models consider modifications in single channel conductances as well as changes in receptor number, but have tended to focus on single synapses or spines. None have considered the consequences of lateral diffusion between spines on synaptic AMPA receptor numbers.

2 Diffusion model

We consider a population of excitatory synapses and their associated dendritic spines distributed along a single dendritic cable of length L, see Fig. 1. There are typically thousands of spines distributed along a single dendrite and a single spine has a size of around 1 μm, which is several orders of magnitude smaller than L (Sorra and Harris 2000). Therefore, we represent the population of spines in terms of a continuous density (number of spines per unit surface area) $\rho(x)$, $0 \le x \le L$, where x denotes axial distance along the dendrite from the soma. The density ρ satisfies the normalization condition $\int_0^L \rho(x)\mathrm{d}x = N/l$, where N is the total number of spines on the dendrite and l is its circumference. For simplicity, we assume throughout that the spine density and intrinsic properties of an individual spine, depend only on distance from the soma so that the cable can be treated as a one-dimensional system. Away from

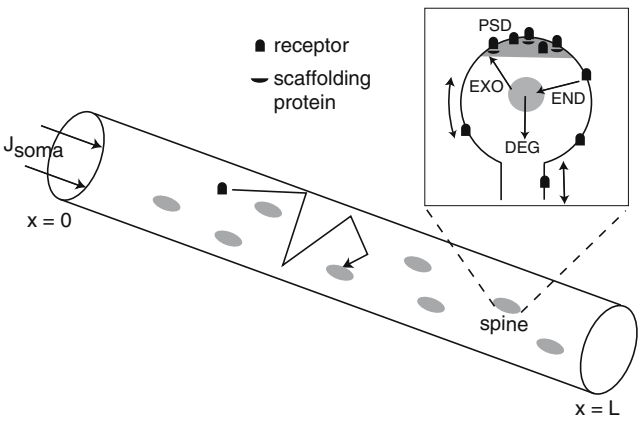

Fig. 1 Diffusion model of AMPA receptor trafficking across multiple synapses. Spines are distributed on the surface of a one-dimensional dendritic cable of circumference l and length L. An AMPA receptor diffuses freely on the surface of the cable with diffusivity D until it encounters a synapse and its associated dendritic spine where it can bind to scaffolding proteins or be internalized into the cell. Surface receptors are internalized via endocytosis (*END*), and then either recycled to the surface via exocytosis (*EXO*) or degraded (*DEG*), see *inset*. Fast exocytosis from the soma generates a surface flux J_{soma} at one end of the cable

a spine, surface AMPA receptors diffuse freely with diffusivity D. Whenever a receptor encounters a dendritic spine, it can flow into the spine and become trapped at the synapse by binding to scaffolding proteins located in the postsynaptic density (PSD) or can be internalized by endocytosis. Internalized receptors can be reinserted into the surface membrane via exocytosis. A schematic illustration of local trafficking within a spine is shown in the inset of Fig. 1. Following Earnshaw and Bressloff (2006), we model each spine as two homogeneous compartments, one corresponding to the PSD and the other to the surrounding extrasynaptic membrane (ESM) of the spine head, see Fig. 2.

Let $U(x,t)$ denote the concentration of dendritic AMPA receptors at position x along the cable at time t. Similarly, let $R(x,t)$ denote the concentration of AMPA receptors within the ESM, and let $P(x,t)$, $Q(x,t)$ denote, respectively, the concentration of unbound and bound AMPA receptors in the PSD of a spine at (x,t). The dendritic AMPA receptor concentration evolves according to the equation

$$\frac{\partial U}{\partial t} = D\frac{\partial^2 U}{\partial x^2} - \rho(x)\Omega(x)[U(x,t) - R(x,t)]. \tag{1}$$

The first term on the right-hand side of Eq. (1) represents the Brownian diffusion of receptors along the surface of the cable. The second term on the right-hand side determines the number of receptors per unit time that flow into or out of a spine at x, which is taken to be proportional to the difference in concentrations across the junction between each spine and the dendritic cable

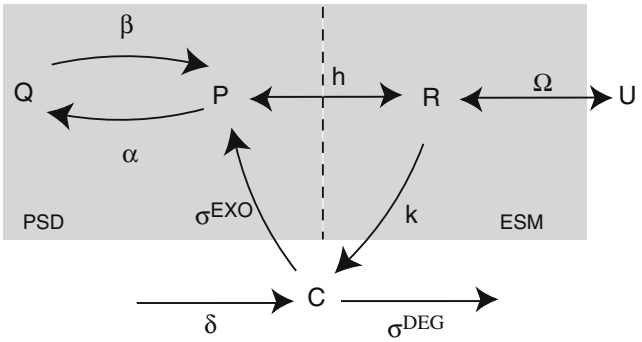

Fig. 2 Simplified two-compartment model of a dendritic spine. Unbound receptors within the PSD (concentration P) bind to scaffolding proteins to form bound receptors (concentration Q) at a rate α (multiplied by the concentration of free binding sites $Z - Q$) and unbind at a rate β. Unbound receptors flow between the PSD and ESM at a hopping rate h, and flow between the ESM (concentration R) and surface of the dendritic cable (concentration U) at a hopping rate Ω. Unbound receptors within the ESM are internalized at a rate k. Receptors are inserted into the PSD from an intracellular pool of C receptors at a rate σ^{EXO} and sorted for degradation at a rate σ^{DEG}. There is also a local production of intracellular receptors at a rate δ

with $\Omega(x)$ an effective hopping rate. Equation (1) is supplemented by boundary conditions at the ends of the cable:

$$D\left.\frac{\partial U}{\partial x}\right|_{x=0} = -J_{\mathrm{soma}}, \quad D\left.\frac{\partial U}{\partial x}\right|_{x=L} = 0. \tag{2}$$

Here J_{soma} represents a constant flux of surface AMPA receptors inserted into the dendrite at the boundary $x = 0$ (adjacent to the soma) arising from somatic exocytosis (Adesnik et al. 2005). The distal end of the cable at $x = L$ is taken to be closed. Note that in a previous model of protein receptor trafficking along a dendrite we considered a discrete population of point-like spines in which the spine density is given by a discrete sum of Dirac delta functions (see Bressloff and Earnshaw 2007 and Appendix 1). In fact one can view the continuum spine model as an approximation of the discrete spine model in the case of a large number of closely spaced spines such that the spine density is approximated by a continuous function. A major advantage of the continuum spine model is that one can use Green's function methods to solve for the dendritic receptor concentration along analogous lines to the standard cable equation (see Section 3). It should also be noted that in our previous analysis (Bressloff and Eranshaw 2007), we considered a simplified one-compartment model of a spine, in which the effects of binding to scaffolding proteins were neglected.

The receptor concentrations within each spine satisfy the equations (Earnshaw and Bressloff 2006)

$$\frac{\partial R}{\partial t} = \frac{1}{A}\left(\Omega[U - R] - kR - h[R - P]\right) \tag{3}$$

$$\frac{\partial P}{\partial t} = \frac{h}{a}[R - P] - \alpha[Z - Q]P + \beta Q + \frac{\sigma}{a} \tag{4}$$

$$\frac{\partial Q}{\partial t} = \alpha[Z - Q]P - \beta Q, \tag{5}$$

where all the single-spine parameters may themselves depend on x (not shown for notational convenience). The first term on the right-hand side of Eq. (3) represents the exchange of AMPA receptors in the ESM with AMPA receptors on the dendritic surface. Since $\Omega[U - R]$ represents the number of AMPA receptors per unit time flowing across the junction between the dendritic cable and ESM, it is necessary to divide through by the surface area A of the ESM in order to properly conserve AMPA receptor numbers. The second term in Eq. (3) represents endocytosis from the ESM at a rate of k receptors per unit time. Our assumption that endocytosis occurs outside but in the vicinity of the PSD is based on a number of experimental studies, see for example Blanpied et al. (2002). The last

term in Eq. (3) and the first term in Eq. (4) represents the exchange of AMPA receptors in the ESM with unbound PSD receptors. Similar to the dendrite-spine exchange, $h[R-P]$ represents the number of AMPA receptors per unit time flowing across the PSD-ESM junction with hopping rate h, and we must divide h by the appropriate surface area in order to conserve AMPA receptor numbers. Here a denotes the surface area of the PSD of a synapse, so that $A+a$ denotes the surface area of the entire spine head. The second term in Eq. (4) and the first term in Eq. (5) represent the binding of unbound PSD AMPA receptors at a rate $\alpha[Z-Q]$, where Z is the concentration of binding sites, $Z-Q$ is the concentration of free binding sites, and α is the binding rate per free binding site. The third term of Eq. (4) and the last term of Eq. (5) represent the unbinding of bound PSD AMPA receptors at a rate β. The last term σ on the right-hand side of Eq. (4) represents the number of receptors inserted into the PSD from an intracellular pool per unit time. Finally, the strength of a synapse is identified with the total number S of PSD AMPA receptors,

$$S = a[P+Q]. \tag{6}$$

This assumes for simplicity that all receptors have the same conductance, and that the size of an EPSP scales linearly with the number of receptors (but see Holmes and Grover 2006).

In our previous single-spine model (Earnshaw and Bressloff 2006) the dendritic concentration U in the vicinity of a spine was fixed at some background level so that Eqs. (3)–(5) became self-contained and independent for each spine. One of the advantages of our multi-spine model is that it allows us to determine U from first principles by solving the diffusion equation (1). However, this now complicates the analysis since lateral diffusion introduces an effective coupling of receptor trafficking between spines.

Another simplification of the previous single-spine model was to take the rate of local receptor insertion σ to be time-independent under basal conditions. This assumes that there exists a local intracellular pool of receptors whose state is maintained either by some form of local receptor synthesis or by the targeted delivery of intracellular receptors transported from the soma along microtubules. The necessary machinery for AMPA receptor synthesis has been found in some dendrites (Pierce et al. 2000), and there is growing evidence that synaptic-plasticity inducing stimuli can promote the local synthesis of proteins (Kelleheler et al. 2004; Ju et al. 2004; Sutton and Schuman 2005). However, it is not yet known whether there exists an activity-independent component to local protein synthesis that contributes to receptor trafficking under basal conditions. If AMPA receptors are primarily synthesized at the soma, then they can be transported to dendritic sites either by lateral diffusion in the plasma membrane (Adesnik et al. 2005) or intracellularly via motor-driven transport along microtubules (Kim and Lisman 2001; Setou et al. 2002). In the latter case this provides a local source of intracellular receptors for delivery to the surface via exocytosis, which supplements the constitutive recycling of receptors via local endosomes (Ehlers 2000). At the simplest level, constitutive recycling within a spine at x can be modeled in terms of the number $C(x,t)$ of receptors in the associated local intracellular pool (Lauffenberger and Linderman 1993):

$$\frac{\partial C}{\partial t} = -\sigma^{\mathrm{EXO}} C - \sigma^{\mathrm{DEG}} C + kR + \delta, \tag{7}$$

where σ^{EXO} is the rate of exocytosis from the intracellular pool, σ^{DEG} is the rate of degradation and kR is the total number of receptors endocytosed from the ESM per second. The final term δ on the right-hand side of Eq. (7) represents the local rate of accumulation of new (rather than recycled) receptors within the intracellular pool supplied, for example, by the targeted delivery of intracellular receptors from the soma (or possibly by local receptor synthesis). All parameters in Eq. (7) may also be x-dependent (not shown for notational convenience).

One simplification of the above model of constitutive recycling is to assume that spines do not share intracellular stores of AMPA receptors. However, Cooney et al. (2002) found that endosomes, the intracellular compartments responsible for the sorting of receptors for recycling or degradation, can be shared by up to 20 spines. Including endosomal sharing in our model would create a potential source of heterosynaptic interaction between spines. However, the range of heterosynaptic interactions arising from endosomal sharing (10–20 μm) is relatively small compared to the interaction range of lateral AMPA receptor diffusion. Moreover, one could reinterpret the spine density $\rho(x)$ in terms of clusters of spines each of which shares a distinct intracellular pool.

One aspect of the single-spine model that we do not carry over to the multi-spine case is to take into account differences in the subunit composition of AMPA receptors. That is, AMPA receptors are heteromers of four subunits GluR1 to GluR4 (Palmer et al. 2005). Each subunit is comprised of an extracellular N-terminal domain, four hydrophobic regions within the plasma membrane named TM1 to TM4, and an intracellular C-terminal domain. TM2 is a cytosolic hairpin loop

which, together with the TM2 region of the other three subunits, forms the cation pore. The C-terminal domain contains a number of phosphorylation sites and conserved sequences that interact with other intracellular proteins such as PSD scaffolding proteins. The subunit composition of an AMPA receptor determines the manner in which it is trafficked, both under basal conditions and during the expression of long-term potentiation (LTP) and long-term depression (LTD), see the review of Bredt and Nicoll (2003). This difference depends on whether the AMPA receptor contains a subunit with a long C-terminal domain (typically GluR1 or GluR4) or is comprised only of subunits with short C-terminal domains (typically GluR2 and GluR3). The majority of AMPA receptors at mature synapses are either GluR1/2 or GluR2/3 heteromers, and these two receptor classes play different trafficking roles under basal and activity-dependent conditions. In particular, at many synapses constitutive recycling involves primarily GluR2/3 receptors whereas the early expression of LTP is thought to involve the rapid insertion of GluR1/2 into the synapse; these are then slowly exchanged with GluR2/3 receptors via constitutive recycling (McCormack 2006). In this paper we focus on receptor trafficking under basal conditions and thus only consider the trafficking of GluR2/3 receptors.

3 Steady state analysis

In the case of time-independent parameters and no external perturbations, the system of Eqs. (1)–(7) converges to a unique steady state obtained by setting all time derivatives to zero. Equation (7) implies that the steady-state rate of insertion into spines at x is

$$\sigma(x) \equiv \sigma^{\mathrm{EXO}}(x)C(x) = \lambda(x)[k(x)R(x) + \delta(x)] \tag{8}$$

where

$$\lambda(x) = \frac{\sigma^{\mathrm{EXO}}(x)}{\sigma^{\mathrm{EXO}}(x) + \sigma^{\mathrm{DEG}}(x)}.$$

Equations (3)–(5) then imply that the steady-state concentrations of bound and unbound PSD receptors are given by

$$P(x) = R(x) + \frac{\sigma(x)}{h(x)}, \quad Q(x) = \frac{\alpha(x)P(x)Z(x)}{\beta(x) + \alpha(x)P(x)} \tag{9}$$

and the concentration of receptors in the ESM is

$$R(x) = \frac{\Omega(x)U(x) + \lambda(x)\delta(x)}{\Omega(x) + k(x)(1-\lambda(x))}. \tag{10}$$

If the dendritic receptor concentration were fixed then Eqs. (9) and (10) would independently hold for each x (as assumed in our previous single-spine model, see Earnshaw and Bressloff 2006). However, $U(x)$ now has to be determined self-consistently by substituting Eq. (10) into the steady-state version of the diffusion equation (1):

$$D\frac{d^2U}{dx^2} - \rho(x)\widehat{\Omega}(x)U(x) = -\rho(x)\widehat{\Omega}(x)r(x), \tag{11}$$

where

$$\widehat{\Omega}(x) = \frac{\Omega(x)k(x)(1-\lambda(x))}{\Omega(x) + k(x)(1-\lambda(x))} \tag{12}$$

and

$$r(x) = \frac{\lambda(x)\delta(x)}{k(x)(1-\lambda(x))} = \frac{\sigma^{\mathrm{EXO}}(x)\delta(x)}{\sigma^{\mathrm{DEG}}(x)k(x)}. \tag{13}$$

One can view $\widehat{\Omega}(x)$ as an effective spine-neck hopping rate and $r(x)$ as an effective ESM receptor concentration. Equation (11) is supplemented by the boundary conditions (2). In the following we solve the steady-steady state diffusion equation (11) for various spine configurations in order to determine how the distribution of synaptic receptors along the dendrite depends on model parameters. In particular, we investigate the efficacy of lateral membrane diffusion in delivering receptors to distal synapses (Section 3.1), and explore how synaptic receptor numbers are modified by local (Section 3.2) or global (Section 3.3) changes in constitutive recycling.

3.1 Distribution of AMPA receptors for uniformly distributed identical spines

The steady-state diffusion equation (11) can be solved explicitly in the special case of identical spines distributed uniformly along the cable. The spine density, the hopping rate between dendrite and spines, and all trafficking parameters associated with constitutive recycling are now x-independent and we can write $\rho(x) = \rho_0$, $\Omega(x) = \Omega_0$, $k(x) = k_0$, $\sigma^{\mathrm{EXO}}(x) = \sigma_0^{\mathrm{EXO}}$, $\sigma^{\mathrm{DEG}}(x) = \sigma_0^{\mathrm{DEG}}$ and $\delta(x) = \delta_0$. Equation (11) then reduces to the simpler form

$$\frac{d^2U}{dx^2} - \Lambda_0^2 U(x) = -\Lambda_0^2 r_0, \tag{14}$$

where

$$\Lambda_0 = \sqrt{\frac{\rho_0\widehat{\Omega}_0}{D}} \tag{15}$$

with

$$r_0 = \frac{\sigma_0^{\mathrm{EXO}}\delta_0}{\sigma_0^{\mathrm{DEG}}k_0}, \quad \widehat{\Omega}_0 = \frac{\Omega_0 k_0(1-\lambda_0)}{\Omega_0 + k_0(1-\lambda_0)} \tag{16}$$

and $\lambda_0 = \sigma_0^{\rm EXO}/(\sigma_0^{\rm EXO} + \sigma_0^{\rm DEG})$. Integrating Eq. (14) with respect to x and using the boundary conditions (2) yields the conservation condition

$$lJ_{\rm soma} = N\widehat{\Omega}_0 \left[\int_0^L U(x)dx/L - r_0 \right].$$

This implies that the total number of receptors entering the dendrite from the soma is equal to the mean number of receptors hopping from the dendrite into the N spines. Note that if there were no degradation of receptors within the intracellular pools ($\sigma_0^{\rm DEG} = 0,\ \lambda_0 = 0$) then $\widehat{\Omega}_0 = 0$ and it would not be possible to satisfy the conservation equation; the number of receptors in the dendrite would grow without bound.

The steady-state diffusion equation (14) can be solved using Green's function methods along similar lines to the standard cable equation describing electrical current flow in passive dendrites (Rall 1962; Tuckwell 1988; Koch 1999) with Λ_0 interpreted as an effective space constant for surface receptor diffusion and transport. Given the boundary conditions (2), the resulting solution for the steady-state dendritic receptor concentration can be written in the form

$$U(x) = \frac{J_{\rm soma}}{D} G(x, 0) + r_0,$$

where G is the one-dimensional Green's function for a cable of length L with closed ends at $x = 0,\ L$:

$$G\left(x, x'\right) = \frac{\cosh\left(\Lambda_0\left[|x - x'| - L\right]\right)}{2\Lambda_0 \sinh(\Lambda_0 L)} + \frac{\cosh\left(\Lambda_0\left[x + x' - L\right]\right)}{2\Lambda_0 \sinh(\Lambda_0 L)}. \quad (17)$$

Hence,

$$U(x) = \frac{J_{\rm soma}}{D} \frac{\cosh(\Lambda_0[x - L])}{\Lambda_0 \sinh(\Lambda_0 L)} + r_0. \quad (18)$$

Assuming that $\Lambda_0 L \ll 1$, we see that the dendritic receptor concentration is an exponentially decaying function of distance x from the soma, asymptotically approaching the uniform background concentration r_0 at a rate Λ_0.

Given the steady-state dendritic receptor concentration $U(x)$, the corresponding distribution of ESM receptors across the population of spines is determined from Eq. (10):

$$R(x) = \frac{\Omega_0 U(x) + \lambda_0 \delta_0}{\Omega_0 + k_0(1 - \lambda_0)}. \quad (19)$$

Clearly, if the spine neck geometry severely restricted the diffusion of spines such that Ω_0 were negligible ie. $\Omega_0 \ll k_0(1 - \lambda_0)$, then each spine would essentially be isolated and $R(x) \approx r_0$ independently of $U(x)$. However, an estimate of Ω_0 based on analyzing diffusion within the spine neck suggests a value of Ω_0 that is not negligible (see Appendix 2 and Table 1). Moreover, experimental data shows that although receptors tend to slow down around the spine neck they are not prevented from entering the spine (Ashby et al. 2006), and hence diffusion within the dendritic membrane needs to be taken into account. We will further assume that under basal conditions the rate of degradation is comparable to the lifetime of an AMPA receptor, which is approximately 1 day (Archibald et al. 1998). This is based on the notion that degradation within intracellular pools is an error-correction mechanism that removes faulty receptors at a rate comparable to the rate at which they occur. Given experimentally measured rates of endo/exocytosis (Luscher et al. 1999; Ehlers 2000; Lin et al. 2000; Passafaro et al. 2001), we thus take $0 < \sigma_0^{\rm DEG} \ll \sigma_0^{\rm EXO}$ such that $\lambda_0 \approx 1$ and

Table 1 Baseline parameter values for dendrite and receptor trafficking

Parameter	Symbol	Value	Units	Reference
Length of dendrite	L	1	mm	Sorra and Harris (2000)
Circumference of dendrite	l	1	μm	Sorra and Harris (2000)
Diffusion coefficient	D	0.1	$\mu m^2 s^{-1}$	Tardin et al. (2003)
Spine density	ρ_0	1	μm^{-2}	Sorra and Harris (2000)
Surface area of ESM	A_0	1	μm^2	Sorra and Harris (2000)
Surface area of PSD	a_0	0.1	μm^2	Sorra and Harris (2000)
Scaffolding protein concentration	Z_0	200	μm^{-2}	Earnshaw and Bressloff (2006)
Binding rate	α_0	10^{-4}	$\mu m^2 s^{-1}$	Earnshaw and Bressloff (2006)
Unbinding rate	β_0	10^{-4}	s^{-1}	Earnshaw and Bressloff (2006)
PSD-ESM hopping rate	h_0	10^{-3}	$\mu m^2\ s^{-1}$	Earnshaw and Bressloff (2006)
ESM-dendrite hopping rate	Ω_0	10^{-3}	$\mu m^2\ s^{-1}$	Earnshaw and Bressloff (2006)
Rate of endocytosis	k_0	10^{-3}	$\mu m^2\ s^{-1}$	Ehlers (2000)
Rate of exocytosis	$\sigma_0^{\rm EXO}$	10^{-3}	s^{-1}	Passafaro et al. (2001)
Degradation rate	$\sigma_0^{\rm DEG}$	10^{-5}	s^{-1}	

$\Omega_0 \gg k_0(1-\lambda_0)$ (see Table 1). It then follows from Eq. (16) that

$$r_0 = \frac{\lambda_0 \delta_0}{(1-\lambda_0)k_0} \gg \frac{\delta_0}{\Omega_0} \tag{20}$$

and, since $U(x) \geq r_0$, Eq. (19) implies that the free receptor concentration in the ESM is approximately equal to the dendritic receptor concentration:

$$R(x) \approx U(x). \tag{21}$$

Moreover, the effective hopping rate $\widehat{\Omega}_0$ is now approximately independent of the bare hopping rate Ω_0,

$$\widehat{\Omega}_0 \approx \frac{k_0 \sigma_0^{\mathrm{DEG}}}{\sigma_0^{\mathrm{EXO}}}, \tag{22}$$

which means that the steady state dendritic receptor concentration $U(x)$ is independent of Ω_0.

It remains to determine the spatial profiles of bound and unbound receptors within the PSD. First, it is important to note that the above solution for $U(x)$ and $R(x)$ still holds even if parameters that specify properties of the PSD are spatially varying, including the area of the PSD, the rates at which receptors bind to and unbind from scaffolding proteins and the concentration of scaffolding proteins. However, in the case of identical spines, we can take these properties to be x-independent and set $\alpha(x) = \alpha_0$, $\beta(x) = \beta_0$, $Z(x) = Z_0$, $h(x) = h_0$ and $a(x) = a_0$. Equations (9), (18) and (21) then imply that the distribution of unbound receptors within the PSD is also exponential-like with

$$P(x) = R(x)\left[1 + \frac{\lambda_0 k_0}{h_0}\right] + \frac{\lambda_0 \delta_0}{h_0}. \tag{23}$$

Finally, Eq. (9) shows that the distribution of bound receptors is

$$Q(x) = \frac{\alpha_0 Z_0 P(x)}{\beta_0 + \alpha_0 P(x)} \tag{24}$$

Hence, the total number of receptors per synapse, $S(x) = a_0(P(x) + Q(x))$, is a monotonically decreasing but possibly non-exponential function of distance x from the soma, due to the nonlinear kinetics associated with binding to scaffolding proteins. For proximal synapses where $P(x)$ is relatively large we expect the binding sites to be saturated, that is,

$$\frac{\alpha_0}{\beta_0} P(x) \gg 1 \text{ such that } Q(x) \approx Z_0.$$

On the other hand, at sufficiently distal synapses and sufficiently small background concentration r_0, synapses will tend to be unsaturated with almost all synaptic receptors bound, $P(x) \ll Q(x) < Z_0$.

In Fig. 3 we plot examples of steady-state receptor distributions for a dendritic cable of length $L = 1$ mm and circumference $l = 1$ μm, containing $N = 1{,}000$ identical spines distributed uniformly along the cable with density $\rho_0 = 1$ μm^{-2} (Sorra and Harris 2000). The baseline values for the various kinetic parameters shown in Fig. 2 are specified in Table 1. Some of these are based on typical values obtained from direct experimental measurements, for example, diffusivity $D = 0.05$–0.5 μm^2 s^{-1} (Borgdorff and Choquet 2002; Tardin et al. 2003; Groc et al. 2004; Ashby et al. 2006) and rates of exo/endocytosis (10–30 min) that are consistent with fast recycling (Luscher et al. 1999; Ehlers 2000; Lin et al. 2000; Passafaro et al. 2001). Other parameters are based on fitting the single-spine model to physiological data (Earnshaw and Bressloff 2006). We then choose the somatic flux so that the maximum number of synaptic receptors per spine lies within the range of 0–200 observed experimentally (Nusser et al. 1998; Cottrell et al. 2000; Tanaka et al. 2005). Figure 3(a, b) show the profiles for dendritic receptor concentration (black curves) and synaptic receptor number per spine (thick gray curves) for two values of the diffusivity ($D = 0.1$ μm^2 s^{-1} and $D = 0.45$ μm^2 s^{-1}), and a nonzero rate of intracellular production ($\delta_0 = 10^{-3}$ s^{-1}). The dendritic receptor concentration decays exponentially (at a rate $\Lambda_0 \approx 0.01$ μm^{-1} for $D = 0.1$ μm^2 s^{-1}) to an asymptotic background level and the rate of decay is smaller for larger diffusivity. For the given choice of parameters, the profile for synaptic receptor number is approximately flat with equal numbers of bound and unbound receptors (as indicated by the thin gray curves), and the binding sites are saturated due to the fact that the background receptor concentration r_0 is sufficiently large. The division of synaptic AMPA receptors into roughly equal proportions of bound and unbound receptors is consistent with data concerning the ratio of mobile and immobile synaptic receptors obtained from both single-particle tracking and FRAP experiments (Groc et al. 2004; Ashby et al. 2006). However, certain care must be taken in identifying mobile and immobile receptors with bound and unbound receptors, respectively, since it is possible that a receptor/scaffolding protein complex could also be partially mobile within the PSD (Choquet and Trillier 2003).

The corresponding profiles for zero intracellular production ($\delta_0 = 0$) are shown in Fig. 3(c, d). In this case the sole source of receptors is from the surface of the soma, and thus the population of receptors within the intracellular pools is maintained by lateral membrane diffusion combined with constitutive recycling. If $\delta_0 = 0$ then Eqs. (16) and (18) imply that the background concentration is zero, $r_0 = 0$, and the dendritic receptor concentration approaches zero towards the distal end at $x = L$. Moreover, the number of unbound

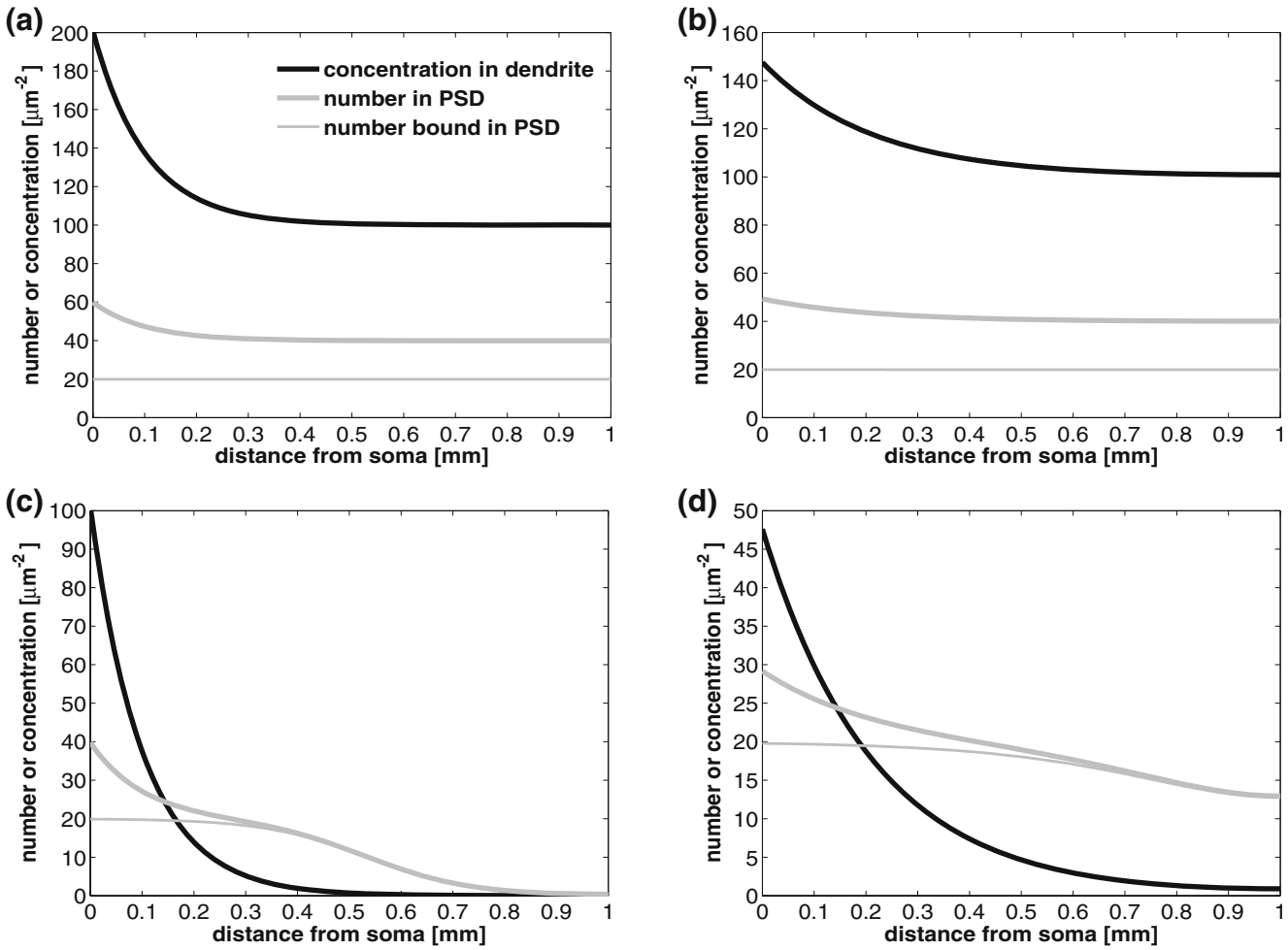

Fig. 3 Steady-state distribution of AMPA receptors as a function of distance x from the soma. The length and circumference of the cable are $L = 1$ mm and $l = 1$ μm. $N = 1{,}000$ identical spines are distributed uniformly along the cable with density $\rho_0 = 1$ μm^{-2}. Unless specified otherwise, all spine parameters are taken to have the baseline values listed in Table 1 and the somatic flux is $J_{\text{soma}} = 0.1$ μm^{-1} s^{-1}. (**a**) Receptor profiles for nonzero local synthesis ($\delta_0 = 10^{-3}$ s^{-1}) and diffusivity $D = 0.1$ μm^2 s^{-1}. The dendritic receptor concentration U (*black curve*) and synaptic receptor number per spine $S = a_0(P + Q)$ (*thick gray curve*) decrease exponentially from the soma. *Thin gray curve* shows number of bound receptors $a_0 Q$ within the PSD. The number of receptors in the ESM and intracellular pools (not shown) is almost exactly the dendritic receptor concentration for the given parameter values. (**b**) Corresponding receptor profiles for diffusivity $D = 0.45$ μm^2 s^{-1}. The profiles are similar to (**a**) except now the rate of exponential decay is slower although the number of synaptic receptors at distal synapses remains the same. (**c**, **d**) Same as (**a**, **b**) except now there is no local production of AMPA receptors ($\delta_0 = 0$)

receptors within the PSD decays sufficiently rapidly so that away from the soma almost all synaptic receptors are bound to scaffolding proteins and the binding sites are no longer saturated. Thus the number of bound receptors also decreases as x increases. For relatively small diffusivity ($D = 0.1$ μm^2 s^{-1}) the dendritic receptor concentration at the distal end is insufficient to maintain receptors within the PSD, whereas it is sufficient for relatively high diffusivity $D = 0.45$ μm^2 s^{-1}. In Fig. 4 we show how the decay rate Λ_0 and the number of synaptic receptors at the distal end (for $\delta_0 = 0$) depend on various parameters. It can be seen that both quantities are sensitive to changes in each parameter. Moreover, for the basal parameter values given in Table 1, $\widehat{\Omega}_0$ can be approximated according to Eq. (22) so that Eq. (15) implies

$$\Lambda_0 \approx \sqrt{\frac{\rho_0 k_0 \sigma_0^{\text{DEG}}}{\sigma_0^{\text{EXO}} D}}.$$

This explains why D and σ_0^{EXO} have similar effects on Λ_0 as do k_0 and σ_0^{DEG}, see Fig. 4(a).

Our steady-state analysis leads to two important results regarding the distribution of AMPA receptors along a dendritic cable. First, our analysis suggests that somatic surface receptors are unlikely to be the sole

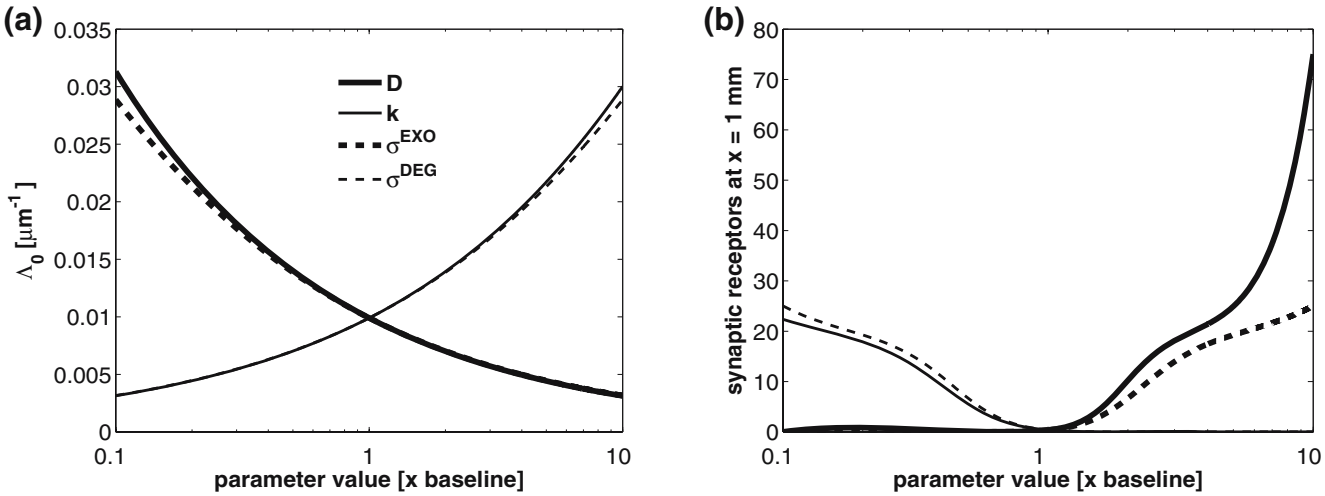

Fig. 4 Properties of steady-state distribution of AMPA receptors along a cable. (**a**) Rate of exponential decay Λ_0 as a function of the diffusivity D and the rates of endocytosis k_0, exocytosis σ_0^{EXO} and degradation σ_0^{DEG}. (**b**) Synaptic receptor number at distal end of cable in the absence of intracellular production ($\delta_0 = 0$) as a function of the same parameters. Same baseline parameters as Fig. 3. Note that the number of synaptic receptors at the distal end is negligible when D and σ_0^{EXO} are below baseline or k_0 and σ_0^{DEG} are above baseline

source of receptors trafficked to distal synapses along a dendrite. This follows immediately from Fig. 4(b), which shows that in the absence of additional sources of receptors ($\delta_0 = 0$), the number of synaptic receptors at distal locations is negligible under basal conditions. This point is further reinforced if one takes into account a well known limitation of diffusion as a molecular transport mechanism, namely, that it tends to be slow. That is, an estimate for the mean time a receptor takes to travel a distance x from the soma via free diffusion within the membrane of a dendritic cable is $\tau = x^2/2D$. For a relatively large diffusivity $D = 0.45$ μm^2 s^{-1}, the mean time to reach a proximal synapse at 100 μm from the soma is of the order 3 h, whereas the time to reach a distal synapse at 1 mm from the soma is of the order 300 h. The latter is much longer than the average lifetime of an AMPA receptor, which is approximately 1 day (Archibald et al. 1998). These simple calculations actually underestimate the mean travel time of a receptor along a dendrite, since they do not take into account the fact that dendritic spines can trap receptors, thus further slowing their progress along a dendrite (Bressloff and Earnshaw 2007). Yet another factor that would tend to slow down the diffusive transport of a receptor is dendritic branching. Therefore, although the constitutive recycling of receptors at synapses could provide a mechanism for allowing viable receptors eventually to reach distal synapses, the fact that diffusive transport is slow does suggest that lateral diffusion is probably supplemented by some form of intracellular motor-driven transport, at least in the case of more distal synapses. Such transport would contribute to a nonzero intracellular production rate, $\delta_0 \neq 0$.

A second result of our analysis is that, given a source of surface receptors at the soma, the receptor concentration in the dendrite and spines tends to be an exponentially decreasing function of distance from the soma, see Fig. 3. Interestingly, there is experimental evidence from CA1 hippocampal neurons suggesting that the spatial profile of the total AMPA receptor concentration along a dendrite is indeed a decaying exponential (Piccini and Malinow 2002). At first sight, such a distribution would appear to bias the strength of synapses towards the proximal end, particularly when the rate of intracellular production is small [see Fig. 3(c, d)], thus contradicting the notion of "synaptic democracy", whereby all synapses of a neuron have a similar capacity for influencing the postsynaptic response regardless of location along a dendritic tree (Hausser 2001; Rumsey and Abbott 2006). Indeed, it has been found experimentally that there is actually an increase in AMPA receptor numbers at more distal synapses (Andrasfalvy and Magee 2001; Magee and Cook 2000), resulting in a distant-dependent variation in synaptic conductance consistent with somatic equalization. Such behavior can be obtained in our model by dropping the assumption of identical spines distributed uniformly along the cable. For it is known that there is a considerable amount of heterogeneity in the properties of spines within a single neuron (reviewed in Nimchinsky et al. 2002). Spine morphology ranges from small filopodial protrusions to large mushroom-like

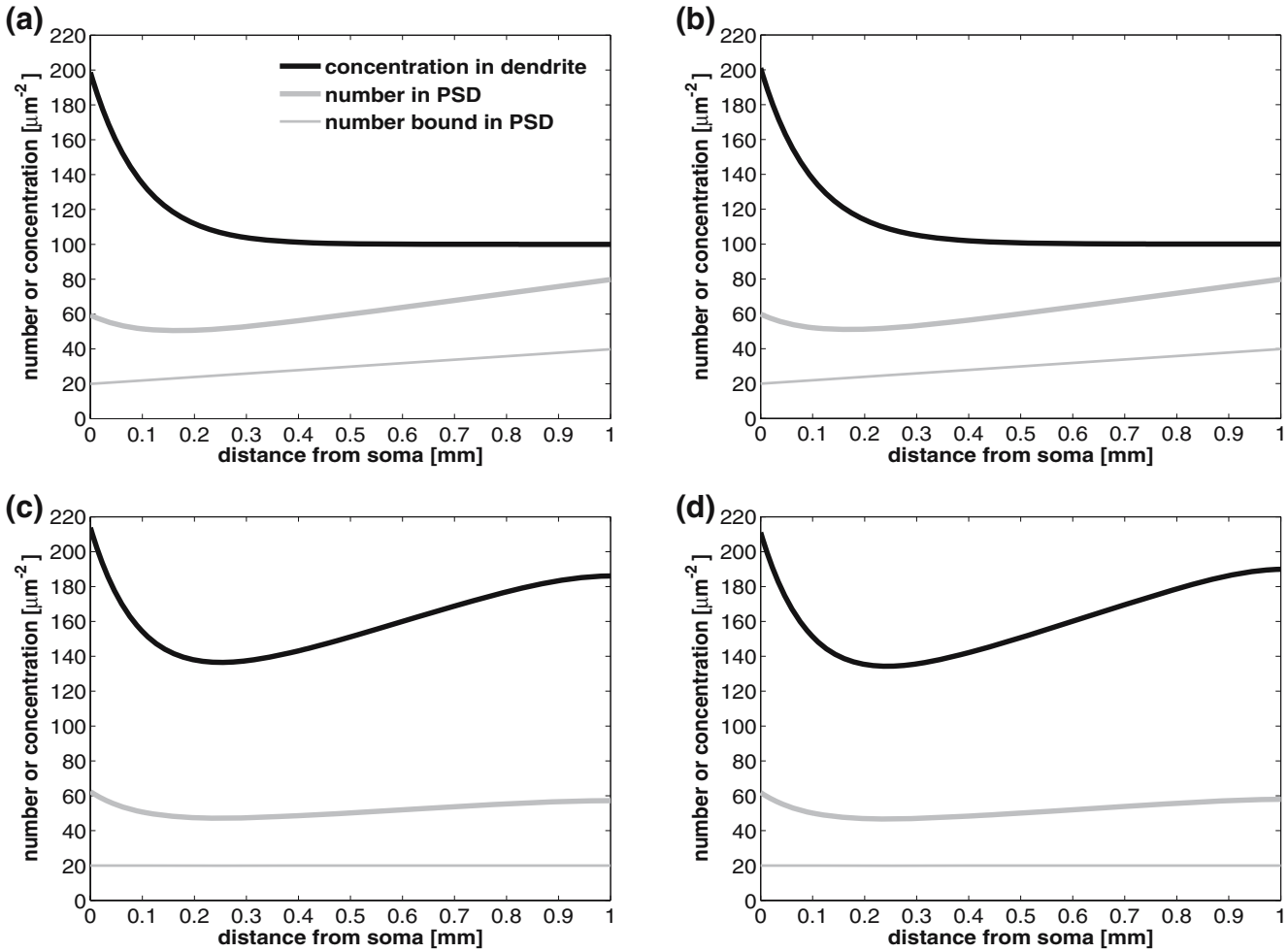

Fig. 5 Steady-state distribution of AMPA receptors as a function of distance x from the soma along a cable with non-identical spines. Parameter values are as in Fig. 3(a) except either (**a**) the surface area a depends on x according to $a(x) = (1 + x/L) \times 10^{-1}$ μm^2, (**b**) the spine density ρ depends on x according to $\rho(x) = (1 + x/L)$ spines μm^{-2}, (**c**) the rate of exocytosis σ^{EXO} depends on x according to $\sigma^{\mathrm{EXO}}(x) = (1 + x/L) \times 10^{-3}$ s^{-1}, or (**d**) the local production rate δ depends on x according to $\delta(x) = (1 + x/L) \times 10^{-3}$ receptors s^{-1}. In each case the number of receptors at distal synapses equals or exceeds receptor numbers at proximal synapses, providing a possible mechanism for synaptic democracy

bulbs, and properties such as the surface area of a spine and spine density tend to vary systematically along the dendrite (Konur et al. 2003). In Fig. 5 we illustrate the effect of having x-dependent parameters in our model. Using parameter values from Fig. 3, in each of Fig. 5(a–d) we vary one of the following parameters y according to $y(x) = y_0(1 + x/L)$, where y_0 is the baseline value from Table 1: the surface area a, the spine density ρ, the rate of exocytosis σ^{EXO} and the local production rate δ. Hence each parameter increases linearly from its baseline value to twice that value at the end of the cable. Note that, in each case, increasing the parameter with distance from the soma allows receptor numbers at distal synapses to match or exceed receptor numbers at proximal synapses, thereby providing a mechanism for synaptic democracy.

3.2 Heterosynaptic interactions mediated by lateral diffusion

One important consequence of lateral membrane diffusion is that one can no longer treat a dendritic spine in isolation. Here we explore the consequences of this by showing how local changes in certain properties of a spine can induce nonlocal changes in the distribution of synaptic receptor numbers along the dendrite. We then interpret our results within the context of heterosynaptic plasticity. A crucial aspect of our analysis is the distinction between single-spine parameters that act nonlocally and those that act locally, which we denote by *extensive* and *intensive* parameters, respectively. Since nonlocal effects are mediated by lateral diffusion, it follows that the extensive parameters are

those that appear in the steady-state diffusion equation (11), namely, the hopping rate through the spine neck Ω and the various parameters associated with constitutive recycling: the rates of exo/endocytosis, degradation and intracellular production ($\sigma^{\rm EXO}$, k, $\sigma^{\rm DEG}$, δ). On the other hand, modifications in the PSD of a spine only effects the number of synaptic receptors within the given spine. Therefore intensive parameters include the area of the PSD a, the rates at which receptors bind to and unbind from scaffolding proteins (α and β), and the concentration of scaffolding proteins Z.

In order to illustrate the nonlocal effects of diffusion, consider a uniform distribution of identical spines and suppose that one or more extensive parameters of the spines at location $x = x_0$ are perturbed. Such a perturbation can be incorporated into the steady-state diffusion equation (11) by setting $\widehat{\Omega}(x) = \widehat{\Omega}_0 + \varepsilon\delta(x - x_0)$, where $\delta(x)$ is the Dirac delta function. For simplicity, we assume that the distribution $r(x) = r_0$ is unperturbed. Equation (11) then becomes

$$\frac{d^2U}{dx^2} - \Lambda_0^2[U(x) - r_0] = \frac{\varepsilon\Lambda_0^2}{\widehat{\Omega}_0}\delta(x - x_0)[U(x) - r_0].$$

In terms of the Green's function (17), this has the formal solution

$$U(x) = \overline{U}(x) - \frac{\varepsilon\Lambda_0^2}{\widehat{\Omega}_0}G(x, x_0)U(x_0),$$

where $\overline{U}(x) = J_{\rm soma}G(x, 0)/D + r_0$ denotes the dendritic receptor concentration for the unperturbed uniform distribution. Setting $x = x_0$ on both sides of this Eq. (3.2) we obtain a closed equation for $U(x_0)$ which can be solved and substituted back into the solution for $U(x)$ to give

$$U(x) = \overline{U}(x)\left[1 - \frac{\frac{\varepsilon\Lambda_0^2}{\widehat{\Omega}_0}G(x, x_0)}{1 + \frac{\varepsilon\Lambda_0^2}{\widehat{\Omega}_0}G(x_0, x_0)}\right].$$

It follows that the induced change in dendritic receptor concentration, $\Delta U(x) = U(x) - \overline{U}$, is maximal at $x = x_0$ and decreases monotonically with distance $|x - x_0|$ at a rate that depends on the space constant Λ_0 defined in Eq. (15). Once $U(x)$ has been calculated, the corresponding changes in synaptic receptor number can be determined from Eqs. (9) and (10).

In Fig. 6 we plot steady-state receptor profiles in response to localized variations in rates of exo/endocytosis or degradation/synthesis. For purposes of illustration we assume that the length of the cable is $L = 200$ μm, that the spine density is again uniform with $\rho_0 = 1$ μm^{-2}, and that there is no somatic flux of receptors, that is, $J_{\rm soma} = 0$. (Including a somatic flux does not alter the basic results other than adding a background exponential decay to the dendritic receptor concentration along the lines of Fig. 3). All spines are assumed to be identical with baseline parameters as in Table 1 except those located 90 to 110 μm from the soma, which employ all baseline parameters except those being perturbed. We first consider the effect of varying the exocytic rate $\sigma^{\rm EXO}$. Increasing $\sigma^{\rm EXO}$ slightly potentiates the number of synaptic receptors of the perturbed and neighboring spines, whereas decreasing $\sigma^{\rm EXO}$ to 0.1 × baseline causes a large depression in the number of synaptic receptors at all spines, see Fig. 6(a). In both cases the number of intracellular receptors within the perturbed region is dramatically different from baseline values, showing the strong dependence of this receptor population on the exocytic rate $\sigma^{\rm EXO}$. Increasing the rate of endocytosis k to 10 × baseline causes synaptic receptor numbers within the perturbed region to increase, whereas all synapses outside this region are depressed, see Fig. 6(b). That an increase in endocytosis leads to an increase in the number of receptors found within the PSD may seem counterintuitive at first sight. However, recall that receptors are not endocytosed from the PSD but from the extrasynaptic region of the spine head. This increases the number of the receptors in the local intracellular pool available to be exocytosed into the PSD, accounting for the increase in synaptic receptors. The opposite effect occurs when k is decreased. Although there is very little change in receptor numbers when the rate of production δ is reduced, all synapses are potentiated when δ is increased (10 × baseline), see Fig. 6(c). The number of intracellular receptors is also increased approximately twofold across all spines. Finally, increasing the rate of degradation $\sigma^{\rm DEG}$ to 10 × baseline depresses all synapses and the number of intracellular receptors now decreases approximately twofold across all spines, see Fig. 6(d).

The results shown in Fig. 6 hold in a parameter regime where the baseline numbers of bound and unbound synaptic receptors are approximately equal. Clearly, if the synapses operate in a saturated regime for which $P(x) \ll Q(x) \approx Z(x)$ then the number of synaptic receptor numbers would be insensitive to heterosynaptic changes in dendritic receptor concentration, provided that the background concentration $P(x)$ was sufficient to maintain synapses in the saturated state.

At first sight, the above analysis suggests that in certain parameter regimes lateral diffusion could lead to some form of heterosynaptic plasticity. That is, suppose we interpret changes in the properties of a spine as a postsynaptic expression mechanism for modifying the number of synaptic AMPA receptors and, hence,

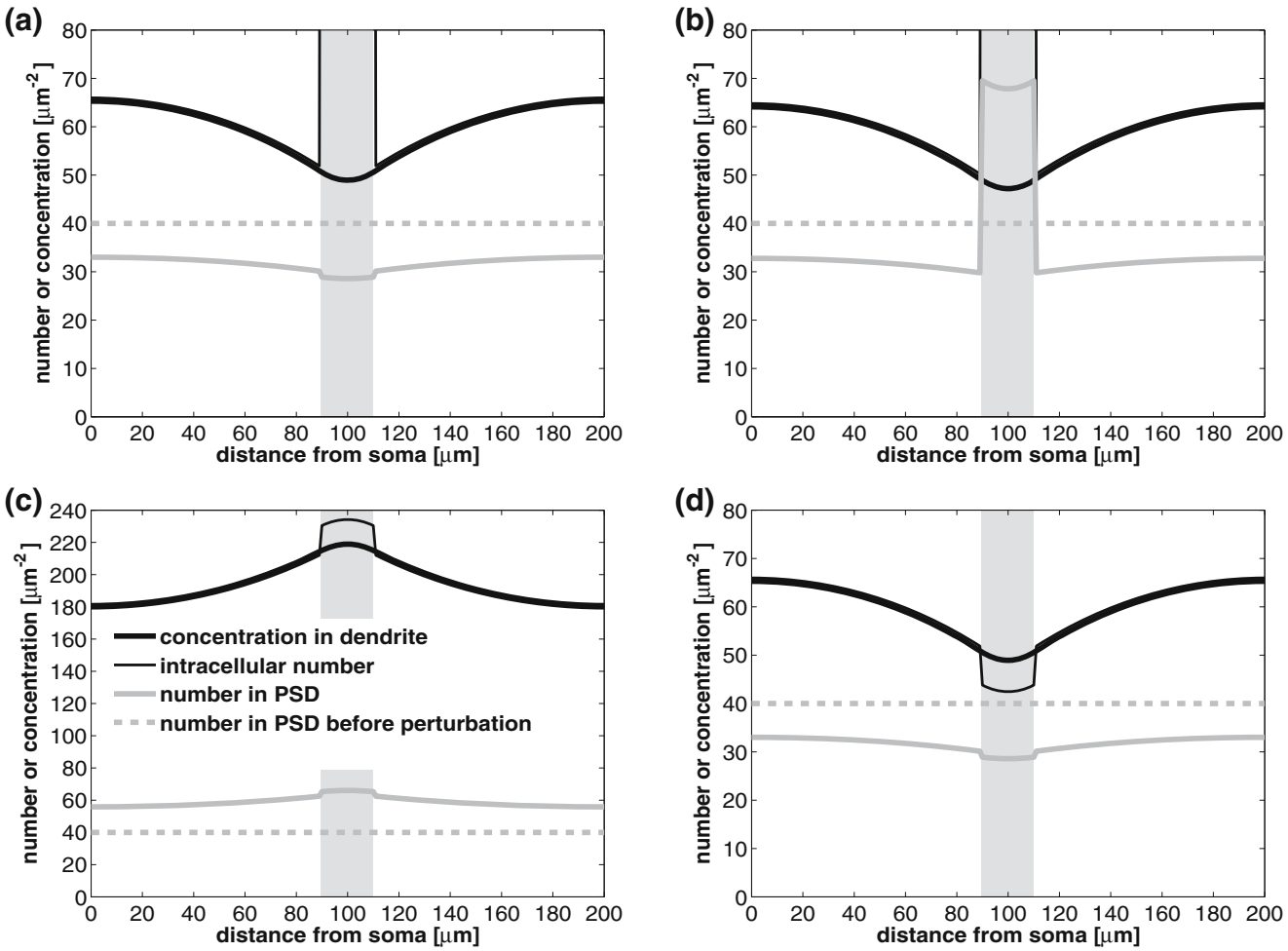

Fig. 6 Nonlocal effects of variations in constitutive recycling. A dendritic cable of length $L = 200$ μm, circumference $l = 1$μm and diffusivity $D = 0.1\mu m^2\ s^{-1}$ has a uniform distribution of spines with density $\rho_0 = 1\ \mu m^{-2}$. All spines are identical, with baseline parameters as in Table 1, except those located 90 to 110 μm from the soma (*shaded gray region*), for which one of the parameters associated with constitutive recycling (σ^{EXO}, k, σ^{DEG}, δ) is perturbed. The resulting steady-state dendritic receptor concentration (*thick black curve*), the number of intracellular receptors (*thin black curve*), and the total number of receptors in the PSD (*thick gray curves*) are plotted as functions of distance x from the soma in response to (**a**) a local reduction in the rate of exocytosis σ^{EXO} (0.1 × baseline), (**b**) a local increase in the rate of endocytosis k (10 × baseline), (**c**) a local increase in the rate of intracellular production δ (10 × baseline), and (**d**) a local increase in the rate of degradation σ^{DEG} (10 × baseline). The total number of synaptic receptors in the absence of the perturbation is indicated by the *dashed gray line*

the strength of the synapse in response to stimulation. If such changes involved extensive parameters then the number of receptors in synapses that are not directly stimulated would also be modified, resulting in a heterosynaptic component to synaptic plasticity arising from lateral diffusion. However, activity-dependent changes associated with the most studied forms of synaptic plasticity, namely long-term potentiation and depression (LTP/LTD), are thought to involve structural changes in the size of the spine and composition of the PSD in order to maintain an increase or decrease in the number of synaptic AMPA receptors (Shi et al. 2001; Malenka and Bear 2004; Matsuzaki et al. 2004; Lamprecht and LeDoux 2004). Such changes primarily involve intensive spine parameters (although structural changes could also result in modifications of the spine neck and, hence, the spine-dendrite hopping rate Ω, any heterosynaptic effects would be small due to the insensitivity of the dendritic receptor concentration to changes in Ω, given the basal parameter values listed in Table 1). Moreover, the various types of heterosynaptic LTP and LTD observed experimentally, either spreading postsynaptically to other synapses on a dendrite or presynaptically to other axon terminals, appear to require some form of long-range chemical signaling, which in the case of postsynaptic spread may involve calcium waves (see the review of Bi and Poo 2001). Hence, it is unlikely that the lateral diffusion of

receptors contributes to experimentally observed forms of heterosynaptic LTP/LTD, at least in the absence of additional signaling mechanisms. This also makes sense computationally, since one would expect plasticity mechanisms to be able to target specific synapses or small clusters of synapses.

3.3 Global scaling of the synaptic receptor distribution and homeostasis

Experimental studies find that a chronic increase/decrease in average cortical activity induces a global and multiplicative scaling of synaptic AMPA receptor-mediated miniature excitatory postsynaptic currents (mEPSCs) in the opposite direction, in order to compensate for the slow cumulative changes in activity (Turrigiano et al. 1998; O'Brien et al. 1998; Turrigiano and Nelson 2004; Davis 2006). Synaptic scaling appears to be associated with an increase or decrease in the number of synaptic AMPA receptors, much like postsynaptic mechanisms for the expression of LTP/LTD. However, the expression of LTP/LTD is faster than synaptic scaling (taking minutes rather than hours) and involves the opposite relationship between neural activity and receptor accumulation. It has been suggested that a global change in the rate of AMPA exocytosis and/or endocytosis could provide the required expression mechanism for synaptic scaling (Turrigiano and Nelson 2004). Here we use our steady-state analysis to investigate the viability of this hypothesis.

An initial examination of Eqs. (9)–(11) implies that the various steady-state receptor concentrations depend nonlinearly on the recycling parameters ($k, \sigma^{\rm EXO}, \sigma^{\rm DEG}, \delta$) so that it is not immediately clear how regulating constitutive recycling leads to a global scaling of synaptic receptor numbers. In order to illustrate this point, suppose that the recycling parameters are uniform along the dendrite, whereas intensive parameters associated with the PSD are allowed to vary so that there is a nonuniform distribution of synaptic receptor numbers. It follows from the form of Eq. (14) that a simple scaling of the dendritic receptor concentration U is not possible unless the variation in the recycling parameters is appropriately constrained. For example, suppose that an up or down regulation of constitutive recycling involves the simultaneous scaling of the exo/endocytic rates by a factor Γ,

$$\sigma_0^{\rm EXO} \to \Gamma \sigma_0^{\rm EXO}, \quad k_0 \to \Gamma k_0,$$

with all other parameters left unchanged. If $\sigma_0^{\rm DEG} \ll \sigma_0^{\rm EXO}$ then both $\widehat{\Omega}_0$ and r_0 are approximately invariant under this scaling, see Eqs. (16) and (22), and it follows from Eq. (14) that the dendritic receptor concentration U is also invariant. Equations (21) and (23) now show that under the above scaling rule, $R(x)$ is scale-invariant and the concentration $P(x)$ of unbound receptors in the PSD undergoes the affine-like transformation

$$P(x) \to \Gamma P(x) + (1-\Gamma) R(x).$$

Since $R(x)$ is generally x-dependent, it is not possible to obtain a global scaling rule for the concentration of unbound receptors within the PSD. The situation is further complicated by the nonlinear relationship between the concentration of bound and unbound receptors within the PSD, see Eq. (9). That is, the total number of synaptic receptors in the PSD of a spine at x is

$$S(x) = a(x) P(x) \left[1 + \frac{\alpha(x) Z(x)}{\beta(x) + \alpha(x) P(x)}, \right]$$

and this clearly does not exhibit global scaling. The failure of modulating constitutive recycling as a mechanism for synaptic scaling is illustrated in Fig. 7, which shows the change in the distribution of synaptic receptor numbers across a dendrite due to a doubling or halving of the rates of exo/endocytosis. Figure 7(a, b) corresponds to the case of identical spines with non-zero somatic flux and zero intracellular production ($\delta = 0$), see Fig. 3(c), whereas Fig. 7(c, d) corresponds to the case of zero somatic flux, non-zero intracellular production and non-identical spines.

In conclusion, even given a number of simplifying assumptions, it does not appear possible to obtain a global multiplicative scaling of synaptic receptor numbers along a dendrite from a simple up or down regulation of constitutive recycling. However, our analysis does suggest an alternative way of regulating the number of synaptic AMPA receptors, namely, by globally scaling the number of binding sites $z(x) \equiv a(x) Z(x)$. That is, suppose the synapses operate in a saturated regime in which most receptors within the PSD are bound so that $P(x) \ll Q(x) \approx Z(x)$ and hence $S(x) \sim z(x)$ [recall from Eq. (6) that S is a receptor number rather than a concentration]. It follows that if $z(x) \to \Gamma z(x)$ then the distribution of synaptic receptors across the dendrite is also scaled multiplicatively, provided that the background dendritic receptor concentration is sufficient to maintain synapses in a saturated state. Interestingly, it has been observed experimentally that receptor accumulation produced by synaptic scaling coincides with global changes in the turnover of many proteins within the PSD that are involved in the clustering of receptors at the synapse including scaffolding proteins (Ehlers 2003). One candidate signaling mechanism for regulating such protein turnover is ubiquitination, which targets proteins for degradation.

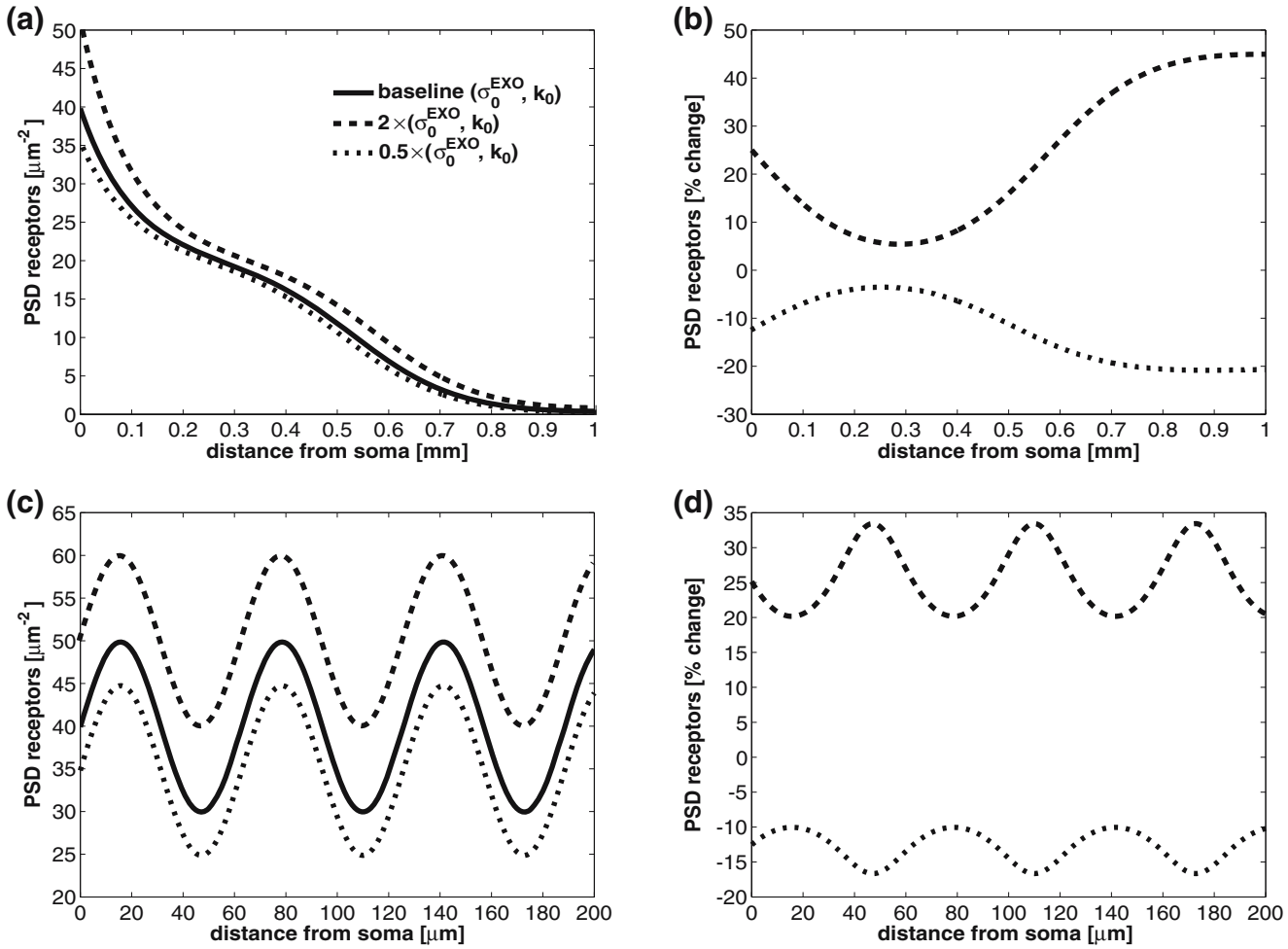

Fig. 7 Global scaling of exo/endocytosis does not imply multiplicative scaling of synaptic AMPA receptor numbers. (**a**) Global scaling for uniform spines, nonzero somatic flux and zero intracellular production. Same parameter values as in Fig. 3(c) unless indicated otherwise. *Solid line* plots baseline number of PSD receptors, *dashed line* plots PSD receptor numbers after a twofold increase in rates of exo/endocytosis ($\sigma_0^{\mathrm{EXO}}, k_0$) and *dotted line* plots PSD receptor numbers after a twofold reduction in these parameters. (**b**) Percent change in PSD receptor numbers from baseline after globally scaling exo/endocytosis as in (**a**). Scaling is not multiplicative as a result of the nonuniform distribution of PSD receptors arising from the nonzero somatic flux J_{soma}. (**c**) Global scaling for nonuniform spines and zero somatic flux. Same parameter values as in Fig. 3(a) except we take the length of the dendrite to be $L = 200$ μm, no somatic flux ($J_{\mathrm{soma}} = 0$), and the concentration of scaffolding proteins to vary as $Z(x) = 100[2 + \sin(x/10)]$. *Solid line* plots baseline number of PSD receptors, *dashed line* plots PSD receptor numbers after a twofold increase in exo/endocytosis ($\sigma_0^{\mathrm{EXO}}, k_0$) and *dotted line* plots PSD receptor numbers after a twofold reduction in these parameters. (**d**) Percent change in PSD receptor numbers from baseline after globally scaling exo/endocytosis as in (**c**). Scaling is not multiplicative as a result of the nonuniform distribution of bound PSD receptors arising from the nonuniform distribution of scaffolding proteins

4 Time-dependent recovery of surface receptor distribution following photoinactivation

So far we have studied steady-state solutions of the reaction–diffusion model given by Eqs. (1)–(7). In particular, we have shown how analytical solutions of the steady-state receptor distributions can be derived by solving an effective cable equation for receptor trafficking. In the case of time-dependent solutions, however, there is no straightforward reduction to a cable equation and it is necessary, in general, to obtain solutions by numerically solving the full system of equations. In this section we use our model to simulate the time-dependent recovery of active surface receptors following photoinactivation (Adesnik et al. 2005), in order to identify the mechanisms that determine the rate of recovery. As we mentioned in the introduction, there are conflicting experimental results regarding the rate of constitutive recycling, which has led to some controversy regarding the major mechanism whereby AMPA receptors are trafficked to dendritic spines. In particular, the relatively fast rate of constitutive

recycling (around 30 min) inferred from a variety of optical, biochemical and electrophysiological studies of hippocampal neurons (Luscher et al. 1999; Ehlers 2000; Lin et al. 2000; Passafaro et al. 2001; Sekine-Aizawa and Huganir 2004) has recently been questioned by the photoinactivation studies of Adesnik et al. (2005), who found that while recovery of surface receptors at the soma is fast, recovery of AMPA receptors at dendritic synapses is much slower (~16 h). These results, combined with similar results obtained in the presence of either the protein synthesis inhibitor cycloheximide or the microtubule-polymerization inhibitor colchicine [which would correspond to taking $\delta_0 = 0$ in Eq. (7)], has led to the proposal that the major source of synaptic receptors arises from the lateral surface diffusion of receptors from the soma. Our steady-state analysis (Section 3) has already suggested that lateral membrane diffusion from the soma is unlikely to be sufficient as a delivery mechanism, at least to distal synapses. Here we use our time-dependent model to show that great care must be taken in interpreting experimental results regarding the rate of recovery following inactivation. In particular, the recovery process can occur on multiple timescales and vary according to location along the dendrite.

We proceed by numerically simulating the time-dependent version of Eqs. (1)–(7) as follows: assuming that all receptor concentrations and numbers are in steady-state (as described in Section 3) for $t < 0$, at time $t = 0$ we instantaneously inactivate all surface receptors in our model. Effectively, this means that we begin tracking these receptors separately from the active receptors, by which we mean those receptors that were in an intracellular pool at time $t = 0$ or are synthesized thereafter. Inactive receptors traffick in the same way as their active counterparts, except that once an inactive receptor is endocytosed we assume that it is sorted for degradation and never reinserted into the neuronal membrane. Only one change is made to Eqs. (4) and (5) and their inactive counterparts: the binding rate is now $\alpha\left[Z - Q - Q^*\right]$, where Q^* is the concentration of bound inactive receptors in the PSD. We expect that the flux J_{soma} of surface receptors from the soma will also be affected by inactivation, hence we take the following simple compartmental model to describe the trafficking of active somatic receptors:

$$\frac{\mathrm{d}R_{\text{soma}}}{\mathrm{d}t} = \sigma_{\text{soma}}^{\text{EXO}} C_{\text{soma}} - (k_{\text{soma}} + \kappa) R_{\text{soma}} \tag{25}$$

$$\frac{dC_{\text{soma}}}{dt} = -\sigma_{\text{soma}}^{\text{EXO}} C_{\text{soma}} + k_{\text{soma}} R_{\text{soma}} + \delta_{\text{soma}} \tag{26}$$

$$J_{\text{soma}} = \kappa R_{\text{soma}}/l, \tag{27}$$

where R_{soma} and C_{soma} are the number of surface and intracellular receptors at the soma, respectively, and $\sigma_{\text{soma}}^{\text{EXO}}$ and k_{soma} are the rates of somatic exo- and endocytosis, respectively. The parameter κ denotes the rate at which somatic surface receptors enter the dendritic membrane, giving rise to form of the flux J_{soma} in Eq. (27). Equations for inactive somatic receptor trafficking are exactly like Eqs. (25)–(27) except that there is no synthesis of inactive receptors ($\delta^*_{\text{soma}} = 0$, where * indicates an inactive trafficking parameter).

In order to implement the numerical simulations of recovery following photoinactivation, we discretize the spatial derivatives in the partial differential equation (1) using a standard finite length method (to conserve receptor numbers) with center differences of step-size 1 μm, and by considering each discretized unit of equation (1) as an ordinary differential equation coupled to both its nearest neighbors along the dendrite. We then use the built-in MatLab solver ode45 to numerically solve the resultant system of ordinary differential equations, composed of the discretized equation (1) together with Eqs. (3)–(7) and (25)–(27), modified to keep track of active and inactive receptors as outlined above.

In Fig. 8 we present the results of our numerical simulations in the case $\delta = 0$, see Eq. (7). That is, there is no local production of AMPA receptors in accordance with the proposal of Adesnik et al. (2005) that synaptic receptors are delivered from the soma via lateral membrane diffusion. For purposes of illustration, we take the dendrite to be 300 μm long and choose all other dendritic parameters as in Fig. 3(c). The corresponding somatic parameters are taken to be $\sigma_{\text{soma}}^{\text{EXO}} = k_{\text{soma}} = 10^{-4}s^{-1}$, $\kappa = 10^{-3}s^{-1}$ and $\delta_{\text{soma}} = 0.1$ receptors s^{-1}. Figure 8(a) shows the steady-state dendritic concentration (black curve) and total and bound number of PSD receptors (thick and thin gray curves, respectively) before inactivation. Note that the fraction of bound receptors in the PSD increases from 50% to 90% with distance from the soma (see inset). In Fig. 8(b) we plot the time course of active PSD receptor numbers at spines 10 μm (solid curves) and 300 μm (dashed curves) from the soma over a period of 24 h following inactivation. We also plot the recovery of active PSD receptor numbers at these locations as a percentage of the number of PSD receptors in each location before inactivation (see insets). The corresponding time courses over the first hour following inactivation are shown in Fig. 8(c). As can be seen from Fig. 8(b) and (c), at 10 μm there is a rapid initial recovery due to the partial replacement of inactive unbound receptors with active receptors from intracellular pools, and a slower recovery thereafter as inactive bound receptors unbind

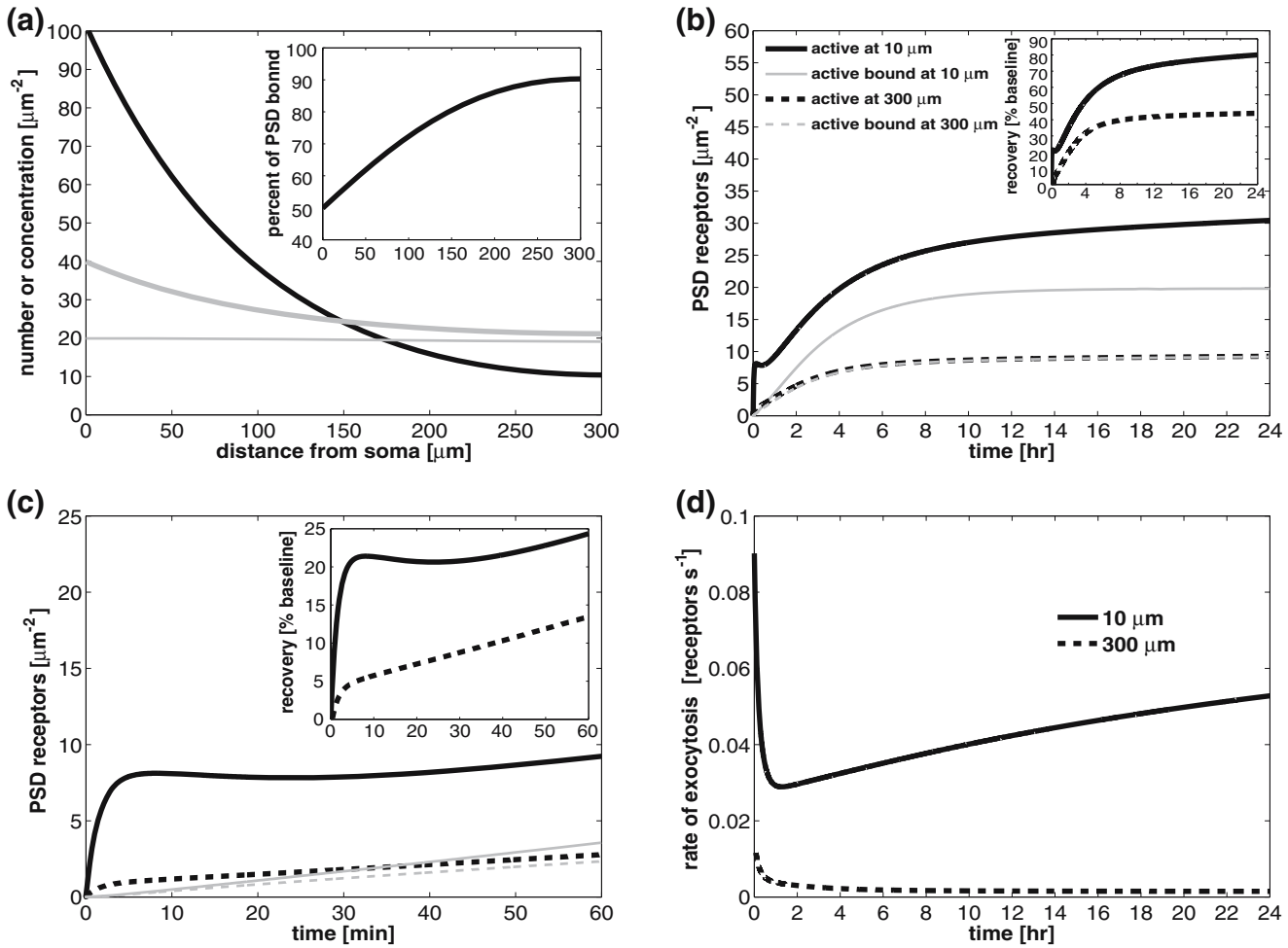

Fig. 8 Recovery of synaptic AMPA receptor numbers after inactivation for $\delta = 0$ (no local intracellular production). We take the dendrite to have length $L = 300$ μm, and all other dendritic parameters as in Fig. 3(c). Somatic parameters for Eqs. (25) and (26) are given in the text. (**a**) Profiles of steady-state dendritic concentration (*black*) and total (*thick gray*) and bound (*thin gray*) PSD numbers before inactivation (*inset* shows percent of PSD receptors bound to scaffolding). (**b**) Recovery of active (*black*) and active bound (*gray*) receptor numbers during the first 24 h after inactivation at PSDs 10 μm (*solid curves*) and 300 μm (*dashed curves*) from the soma (*inset* shows recovery as percentage of pre-inactivation numbers). (**c**) Corresponding time courses during the first hr after inactivation. (**d**) Number of intracellular receptors inserted per second into the PSDs at 10 (*solid*) and 300 (*dashed*) μm from the soma

from scaffolding and are replaced by active ones. At 300 μm, however, recovery is much slower due to two related factors: (1) the fraction of unbound receptors in the PSD is much smaller and (2) there is a slower rate of receptor insertion due to smaller intracellular pools. The latter point is further illustrated in Fig. 8(d), where we plot the number of receptors per second exocytosed into PSDs at both locations, $\sigma(x,t) = \sigma^{\mathrm{EXO}}(x)C(x,t)$. At time $t = 0$ there are nearly 100 receptors in the local intracellular pools at 10 μm compared to 10 at 300 μm, giving rise to the order of magnitude difference in both the rates of receptor insertion and the numbers of unbound receptors at these two locations. After inactivation both insertion rates drop significantly as local intracellular pools are partially depleted while supplying active receptors to the dendritic surface. The initial order of magnitude difference in the rates explains the large initial increase at 10 μm compared to that at 300 μm. After this transient decrease in the rates of insertion, at 10 μm the rate begins increasing again while at 300 μm the rate continues to decrease. This is because receptors diffusing laterally from the soma enter spines at 10 μm relatively quickly and begin replenishing the intracellular stores there, while spines at 300 μm do not receive a single receptor from the soma during the entire 24 h simulation. Having a larger rate of receptor insertion at 10 μm compared to 300 μm provides for more unbound PSD receptors [compare Fig. 8(b, c)], hence a faster rate of binding and ultimately a more rapid recovery.

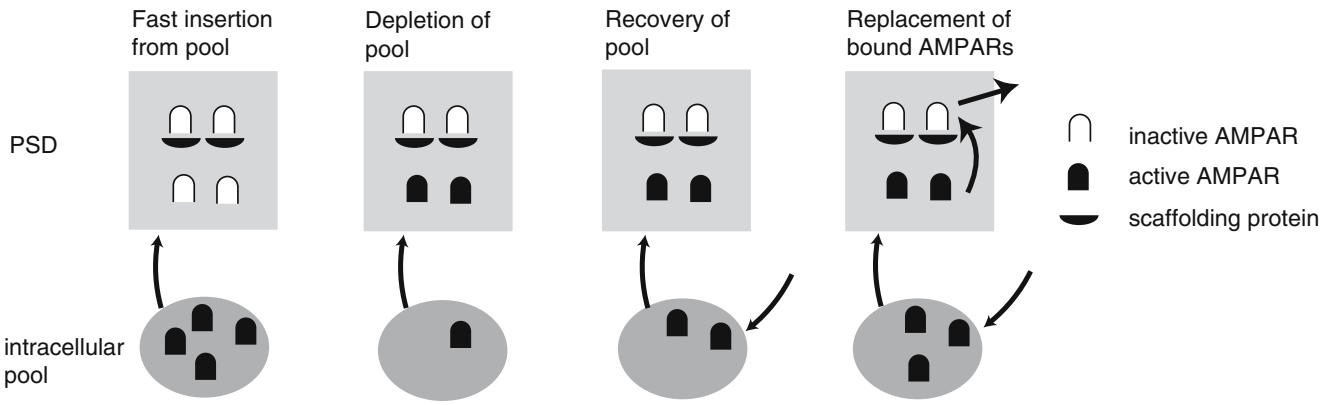

Fig. 9 Various processes contributing to recovery of surface AMPA receptors within the PSD following inactivation (see text for details). Note that there are two distinct mechanisms for recovery of the intracellular pool. The first involves a direct resupplying of the pool via motor-assisted transport of active receptors from the soma possibly combined with local protein synthesis; we model these processes in terms of a nonzero production rate δ, see Eq. (7). The other mechanism occurs via lateral membrane diffusion of active receptors from the soma to dendritic spines combined with constitutive recycling. For simplicity, we have not shown the ESM

The various processes that contribute to the recovery of activity following inactivation are summarized in Fig. 9; the relative importance of these different contributions depends on the distance of a spine from the soma. An initial fast component of recovery arises from the rapid insertion of active unbound receptors from intracellular pools. This then induces a depletion of the pools that may lead to a transient dip in recovery. In order to maintain the long-term recovery of unbound synaptic receptors it is necessary to resupply the intracellular pools; in the absence of local production ($\delta = 0$), this occurs via lateral membrane diffusion of active receptors from the soma. Finally, there is also a slow component of recovery associated with the replacement of bound inactive receptors by active ones. All of these factors contribute to recovery at proximal synapses, whereas only the slow component is found at distal synapses (when $\delta = 0$). It is now straightforward to deduce what happens when local intracellular production is nonzero ($\delta \neq 0$). In this case distal synapses have a significant fraction of unbound receptors in steady-state due to well-stocked intracellular pools. Thus recovery is approximately uniform along the dendrite (assuming uniformly distributed identical spines as in Fig. 3), and consists of fast and slow components corresponding to the recovery of active unbound and bound receptors, respectively. This is illustrated in Fig. 10.

In conclusion, our numerical studies suggest that a number of distinct factors contribute to the recovery of activity following photoinactivation of surface receptors, including the rate at which new receptors are inserted into the PSD from intracellular pools, the rate of refilling of the intracellular pools, and the rate at which receptors unbind from scaffolding proteins (see Fig. 9). It follows that recovery occurs on multiple timescales and varies according to spatial location along the dendrite. Understanding the dynamics of receptor trafficking is thus important when interpreting data from inactivation experiments and inferring values for relaxation time constants associated, for example, with constitutive recycling.

5 Discussion

In this paper we have extended our recent model of AMPA receptor trafficking at a single dendritic spine (Earnshaw and Bressloff 2006) to the case of trafficking across multiple dendritic spines distributed along a dendrite. Unlike our single-spine model, this extension allows us to calculate self-consistently the concentration of dendritic AMPA receptors just outside a spine, given receptor concentrations at all other locations of the dendrite. Since the trafficking of dendritic AMPA receptors is a major determinant of the trafficking of AMPA receptors within each spine, our extension provides a more accurate framework in which to study AMPA receptor trafficking. One of the interesting features of our multi-spine model is that the effects of lateral diffusion in steady state can be described mathematically in terms of an effective cable equation for receptor trafficking. This means that many of the mathematical and numerical techniques previously developed for studying the passive electrical properties of dendrites (see eg. Tuckwell 1988; Koch 1999) can be

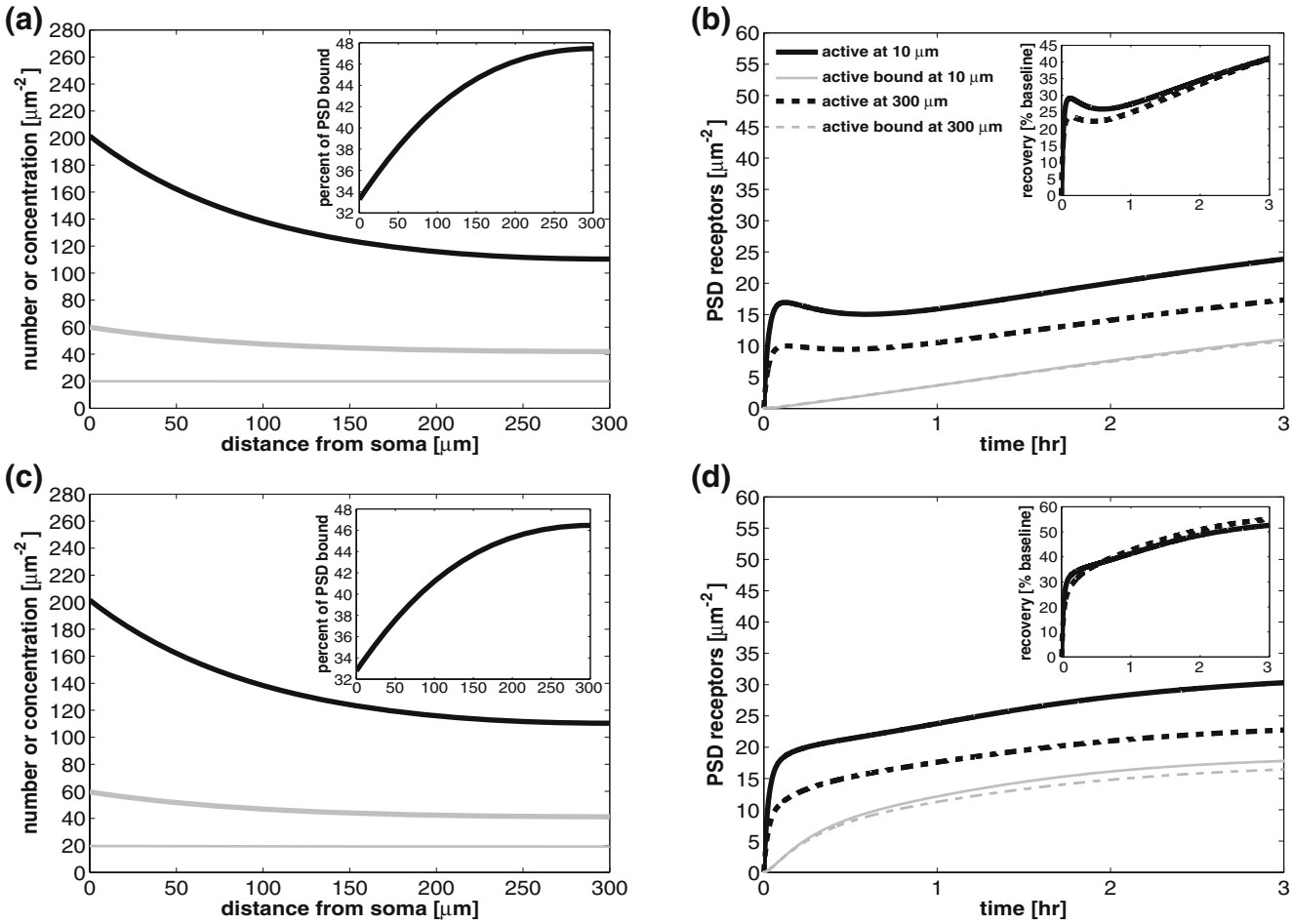

Fig. 10 Recovery of synaptic AMPA receptor numbers after inactivation for $\delta \neq 0$ (nonzero local intracellular production) and different values of unbinding rate β_0, see Eqs. (5) and (7). All other parameters as in Fig. 8. (**a**, **c**) Profiles of steady-state dendritic concentration (*black*) and total (*thick gray*) and bound (*thin gray*) PSD numbers before inactivation for $\beta_0 = 10^{-4} s^{-1}$ and $\beta_0 = 10^{-3}$ s^{-1}, respectively (*insets* show percent of PSD receptors bound to scaffolding). (**b**, **d**) Recovery of active (*black*) and active bound (*gray*) receptor numbers during the first 3 h after inactivation at PSDs 10 μm (*solid curves*) and 300 μm (*dashed curves*) from the soma for $\beta_0 = 10^{-4}$ s^{-1} and $\beta_0 = 10^{-3}$ s^{-1}, respectively (*insets* show recovery as percentage of pre-inactivation numbers). Note that recovery at proximal and distal synapses are now similar. Increasing the rate of unbinding does not affect the steady-state receptor profiles but increases the rate of the slow component of recovery

applied to receptor trafficking, including the effects of branching and spatial inhomogeneities.

One of the main results of our steady-state analysis is to show how various model parameters that control receptor trafficking into and out of a synapse can be classified according to their degree of local versus non-local influence on steady-state synaptic receptor numbers. For example, a change in the number and/or affinity of scaffolding proteins within the PSD has a purely local effect, whereas a variation in the rates of receptor exo/endocytosis has a non-local effect whose range depends on the membrane diffusivity of the dendrite. Interestingly, a global change in the rates of exo/endocytosis does not result in a multiplicative scaling of synaptic receptor numbers along the dendrite, suggesting that is unlikely by itself to provide an expression mechanism for homeostatic synaptic scaling.

Another important issue addressed by our model is the role of surface diffusion in delivering newly synthesized receptors from the soma to dendritic spines. One immediate consequence of having a source of surface receptors at the soma is that it tends to generate an exponentially decaying distribution of receptors along the surface of the dendrite, so that distal synapses cannot be supplied unless diffusivity is sufficiently fast. Moreover, a simple estimate of the mean first passage time for a surface receptor to travel from the soma to a distal location on the dendrite suggests that diffusion is likely to be supplemented by active transport along microtubules. One of the experimental motivations for

considering diffusion as an important delivery mechanism is the slow recovery of active surface receptors following photoinactivation (Adesnik et al. 2005). Numerical simulations of our full time-dependent model suggest that the rate of recovery depends on a number of factors including the fraction of unbound receptors within the PSD, the size of intracellular pools and the rate of unbinding from scaffolding proteins.

An interesting extension of our model would be to consider how receptor trafficking across multiple synapses contributes to forms of synaptic plasticity such as LTP and LTD. In discussing LTP/LTD it is important to distinguish between the various chemical signaling cascades that induce plasticity in response to stimulation, and the subsequent targets of these signals during the expression of synaptic plasticity. That is, whereas a rise in calcium concentration within a dendritic spine is thought to be a crucial induction signal for LTP/LTD, AMPA receptor trafficking is thought to be one of the major targets for the expression of LTP/LTD (Bredt and Nicoll 2003; Malenka and Bear 2004). There is also a separation of time-scales between induction and expression, with the former typically taking seconds and the latter taking minutes. In our previous work on the single-spine model (Earnshaw and Bressloff 2006), we considered various trafficking scenarios during the expression of LTP/LTD and identified changes in the number of scaffolding proteins as a possible mechanism for modifying the strength of a synapse, following the "slot" hypothesis of Shi et al. (2001). With regards to our multi-synapse model, this would not lead to any heterosynaptic effects unless there were some "spillover" associated with the delivery of slot proteins to spines. Experimental studies of heterosynaptic LTP/LTD suggest that they require some form of chemical signal that propagates along a dendrite, at least in the case of postsynaptically spreading LTP/LTD (see the review of Bi and Poo 2001). Thus coupling receptor diffusion with a propagating chemical signal such as a calcium wave might provide a basis for modeling postsynaptic forms of heterosynaptic plasticity.

It is important to note that in order to make our model analytically tractable, we have made a number of simplifying assumptions which we summarize here. First, we treat surface diffusion along the dendritic cable as a one-dimensional process. This can be justified rigorously by considering a full two-dimensional model of diffusion along the cylindrical surface of a dendritic cable with spines treated as small trapping regions. Since the Green's function associated with two-dimensional diffusion has a logarithmic singularity, one has to use singular perturbation theory in order to analyze surface diffusion along a cylinder with small holes (Bressloff et al. 2007). It turns out that since dendrites are long and thin with a large number of spines, the behavior of the two-dimensional model is indistinguishable from the simpler one-dimensional model and, in particular, variations of dendritic receptor concentration around the circumference of the cable are negligible. In the reduced one-dimensional model we can then treat spines as point-like sources such that the spine density consists of a discrete sum of Dirac delta functions, see Appendix 1. The continuum model is then obtained by approximating the density by a continuous function, which is reasonable in the case of a large number of closely spaced spines.

One of the major simplifications at the single spine level is to ignore the effects of diffusion within the PSD and ESM (Earnshaw and Bressloff 2006). This is motivated by the observation that given physiologically reasonable values for the diffusivity of mobile receptors in each of the compartments (Groc 2004), lateral membrane diffusion is relatively fast. In particular, the fluxes involved in receptor trafficking can be maintained by small concentration gradients so that the distribution of receptors within a compartment is approximately spatially uniform. One important aspect of dendritic spines that a diffusion-based single spine model could take into account is the effect of spine geometry on receptor-trafficking, in particular the role of the spine neck in restricting the flow of receptors from the ESM to the dendritic shaft, as recently observed experimentally (Ashby et al. 2006). In our simplified model we represent the effect of the spine neck phenomenologically as an effective hopping rate Ω. However, Ω can be estimated by considering diffusion within the spine neck as shown in Appendix 2.

In treating the PSD (and ESM) as a homogeneous compartment we are effectively carrying out a form of homogenization. In particular, we are neglecting details regarding the interaction of AMPA receptors with scaffolding proteins and cytoskeletal elements within the PSD. Although many scaffolding-related proteins have been identified (Song and Huganir 2002), little is known about how these proteins act in concert to regulate and maintain AMPA receptor numbers at synapses. Hence, we model these proteins phenomenologically in terms of binding sites, which represent complexes able to immobilize AMPA receptors, much like the slot proteins hypothesized by Shi et al. (2001). Another simplification is to assume that escape from the PSD can be represented as a simple hopping process. An alternative model of confinement is to assume that the boundary

between the PSD and ESM is impermeable except for small openings within the boundary through which receptors can diffuse (Holcman and Schuss 2004).

Finally, in our single-spine model we represent the state of a synapse in terms of the concentration of bound and unbound receptors within the PSD. The single-spine dynamics is then formulated in terms of a system of kinetic equations describing the temporal variation of these receptor concentrations, coupled to those in the remaining spine and dendrite. In order for this to be a good description of a single synapse, the number of receptors within the synapse has to be sufficiently large, otherwise random fluctuations about the mean receptor number can become significant, with the mean identified as the synaptic receptor concentration times the area of the PSD. Typically the size of fluctuations varies as $1/\sqrt{N}$ where N is the number of synaptic receptors. One way to determine both the mean and variance of the receptor number is to replace the kinetic equations by a corresponding master equation (van Kampen 1992), which describes the temporal evolution of the probability distribution for the receptors within the spine. For fixed values of the various trafficking parameters, the resulting fluctuations reflect the inherent stochasticity or intrinsic noise of receptor trafficking. An interesting problem is then how to couple the single-spine master equation to diffusion within the dendrite in order to develop a fully stochastic model of receptor trafficking across multiple spines.

Acknowledgements This work was supported by the National Science Foundation (DMS 0515725 and RTG 0354259).

Appendix 1

The diffusion model given by Eq. (1) can be viewed as a continuum approximation of a previous model of protein receptor trafficking along a dendrite, in which lateral diffusion is coupled to a discrete population of spines (Bressloff and Earnshaw 2007). The latter is obtained by taking the spine density to have the explicit form

$$\rho(x) = \frac{1}{l}\sum_{j=1}^{N} \delta\left(x - x_j\right), \tag{28}$$

where $\delta(x)$ is the Dirac delta function and x_j is the distance of the jth spine from the soma. Substitution into Eq. (1) gives

$$\frac{\partial U}{\partial t} = D\frac{\partial^2 U}{\partial x^2} - \sum_{j=1}^{N} \frac{\Omega_j}{l}\left[U_j(t) - R_j(t)\right]\delta\left(x - x_j\right), \tag{29}$$

where $\Omega_j = \Omega(x_j)$, $U_j(t) = U(x_j, t)$ and $R_j = R(x_j, t)$. Note that this discrete spine model ignores the spatial extent of each spine so that the domain over which free diffusion occurs is the whole cylindrical surface of the dendrite. This is motivated by the observation that the spine neck, which forms the junction between a synapse and its parent dendrite, varies in radius from ~ 0.02–0.2 μm, which is typically an order of magnitude smaller than the spacing between spines (∼0.1–1 μm) and the circumference of the dendritic cable (∼1 μm), see Sorra and Harris (2000). In other words, the disc-like region or hole forming the junction between a spine and the dendritic cable is relatively small, and can therefore be neglected in a one-dimensional cable model. As noted in the discussion, In the case of a full two-dimensional model of diffusion along the cylindrical surface of a dendritic cable, one can no longer ignore the effects of these holes due to the fact that the Green's function associated with two-dimensional diffusion has a logarithmic singularity (Bressloff et al. 2007).

For the given spine density (28), the steady-state diffusion equation (11) reduces to

$$0 = D\frac{d^2U}{dx^2} - \sum_{j=1}^{N} \widehat{\Omega}_j\left[U_j - r_j\right]\delta\left(x - x_j\right), \tag{30}$$

where $r_j = r(x_j)$ etc. Integrating Eq. (30) over the interval $0 \le x \le L$ leads to the conservation condition

$$lJ_{\text{soma}} = \sum_{j=1}^{N} \widehat{\Omega}_j\left[U_j - r_j\right] \tag{31}$$

Equation (30) can be solved in terms of the generalized one-dimensional Green's function $H(x, x')$, defined according to the solution of the equation

$$\frac{d^2H\left(x, x'\right)}{dx^2} = -\delta\left(x - x'\right) + L^{-1}, \tag{32}$$

with reflecting boundary conditions at the ends $x = 0$, L. A standard calculation shows that

$$H(x, x') = \frac{L}{12}\left[g\left(\left[x + x'\right]/L\right) + g\left(|x - x'|/L\right)\right], \tag{33}$$

where $g(x) = 3x^2 - 6|x| + 2$. Given the Green's function H, the dendritic surface receptor concentration has an implicit solution of the form

$$U(x) = \chi - \sum_{j=1}^{N} \frac{\widehat{\Omega}_j\left[U_j - r_j\right]}{lD} H\left(x, x_j\right) + \frac{J_{\text{soma}}}{D} H(x, 0), \tag{34}$$

where the constant χ is determined from the conservation condition (31).

We can now generate a matrix equation for the concentration of dendritic receptors U_i at the i^{th} spine, $i = 1, \ldots, N$, by setting $x = x_i$ in Eq. (34):

$$U_i = \chi - \sum_{j=1}^{N} \mathcal{H}_{ij}\left[U_j - r_j\right] + J_i, \tag{35}$$

where

$$\mathcal{H}_{ij} = \frac{\widehat{\Omega}_j}{lD} H\left(x_i, x_j\right), \quad J_i = \frac{J_{\text{soma}}}{D} H(x_i, 0). \tag{36}$$

If the matrix $\mathcal{H} = (\mathcal{H}_{ij})$ does not have -1 as an eigenvalue (which is the generic case), then the matrix $\mathcal{I} + \mathcal{H}$, where $\mathcal{I}$ is the $N \times N$ identity matrix, is invertible and we can solve the system (35). That is, setting $\mathcal{M} = (\mathcal{I} + \mathcal{H})^{-1}$, we have

$$U_i - r_i = \sum_j \mathcal{M}_{ij}\left[\chi + J_j - r_j\right]. \tag{37}$$

The conservation condition (31) then determines χ according to

$$\chi = \left[\frac{lJ_{\text{soma}} - \sum_{k,l} \widehat{\Omega}_k \mathcal{M}_{kl}[J_l - r_l]}{\sum_{k,l} \widehat{\Omega}_k \mathcal{M}_{kl}}\right]. \tag{38}$$

Equations (37) and (38) determine the dendritic receptor concentration U_j at the discrete site x_j of the jth dendritic spine. Substituting this solution into Eq. (34) then generates the full receptor concentration profile $U(x)$. For a large number of spines distributed along a dendrite, the resulting solution matches that obtained from the continuum model of Section 2. Treating the spines as a continuous population makes the analysis more transparent than the matrix solution of the discrete model. For example, it generates a simple expression for the effective space constant of receptor diffusion.

Appendix 2

Here we provide a rough estimate for the hopping rate Ω_0 based on diffusion through the spine neck. For purposes of illustration, let us assume that the spine neck is a uniform cylinder of length L_n and radius r_n. Consider the steady state diffusion equation along the surface of the cylinder:

$$D_n \frac{d^2 U_n}{ds^2} = 0, \quad s \in (0, L_n). \tag{39}$$

with boundary conditions

$$U_n(0) = U, \quad U_n(L_n) = R,$$

where U is the dendritic receptor concentration at the junction between the spine neck and cable and R is the receptor concentration within the ESM. Denoting the constant flux through the spine neck by J_n, we can solve Eq. (39) to obtain

$$U - R = \frac{J_n L_n}{D_n}. \tag{40}$$

Given that the total number of receptors per unit time flowing across either end of the spine neck is $2\pi r_n J_n$, we deduce that

$$\Omega_0 = \frac{2\pi r_n D_n}{L_n}. \tag{41}$$

Using $L_n = 0.45$ μm and $r_n = 0.075$ μm (Sorra and Harris 2000) and $D_n = 6.7 \times 10^{-3}$ μm^{2}s^{-1} (Ashby et al. 2006), we find that $\Omega \approx 7 \times 10^{-3}$ μm^{2}s^{-1}, which is consistent with the baseline value shown in Table 1.

References

Adesnik, H., Nicoll, R. A., & England, P. M. (2005). Photoinactivation of native AMPA receptors reveals their real-time trafficking. *Neuron, 48*, 977–985.

Andrasfalvy, B. K., & Magee, J. C. (2001). Distance-dependent increase in AMPA receptor number in the dendrites of adult hippocampal CA1 pyramidal neurons. *Journal of Neuroscience, 21*, 9151–9159.

Archibald, K., Perry, M. J., Molnar, E., & Henley, J. M. (1998). Surface expression and metabolic half-life of AMPA receptors in cultured rat cerebellar granule cells. *Journal of Neuropharmacology, 37*, 1345–1353.

Ashby, M. C., Maier, S. R., Nishimune, A., & Henley, J. M. (2006). Lateral diffusion drives constitutive exchange of AMPA receptors at dendritic spines and is regulated by spine morphology. *Journal of Neuroscience, 26*, 7046–7055.

Bi, G-Q., & Poo, M-M. (2001). Synaptic modification by correlated activity: Hebb's postulate revisited. *Annual Reviews of Neuroscience, 24*, 139–166.

Blanpied, T. A., Scott, D. B., & Ehlers, M. D. (2002). Dynamics and regulation of clathrin coats at specialized endocytic zones of dendrites and spines. *Neuron, 36*, 435–449.

Bliss, T. V. P., & Lomo, T. (1973). Long-lasting potentiation of synaptic transmission in the dentate area of the anaesthetized rabbit following stimulation of the perforant path. *Journal of Physiology, 232*, 331–356.

Borgdorff, A., & Choquet, D. (2002). Regulation of AMPA receptor lateral movement. *Nature, 417*, 649–653.

Bredt, D. S., & Nicoll, R. A. (2003). AMPA receptor trafficking at excitatory synapses. *Neuron, 40*, 361–379.

Bressloff, P. C., & Earnshaw, B. A. (2007). Diffusion-trapping model of protein trafficking in dendrites. *Physical Review E, 75*, 041916.

Bressloff, P. C., Earnshaw, B. A., & Ward, M. J. (2007). Diffusion of protein receptors on a cylindrical dendritic membrane with partially absorbing traps. *SIAM Journal on Applied Mathematics*, (in press).

Castellani, G. C., Quinlan, E. M., Cooper, L. N., & Shouval, H. Z. (2001). A biophysical model of bidirectional plasticity: dependence on AMPA and NMDA receptors. *Proceedings*

of the National Academy of Sciences of the United States of America, 98, 12772–12777.
Chen, L., Tracy, T., & Nam, C. I. (2007). Dynamics of postsynaptic glutamate receptor targeting. *Current Opinion in Neurobiology, 17*, 53–58.
Choquet, D., & Trillier, A. (2003). The role of receptor diffusion in the organization of the postsynaptic membrane. *Nature Reviews, Neuroscience, 4*, 251–265.
Collingridge, G. L., Isaac, J. T. R., & Wang, Y. T. (2004). Receptor trafficking and synaptic plasticity. *Nature Reviews, Neuroscience, 5*, 952–962.
Cooney, J. R., Hurlburt, J. L., Selig, D. K., Harris, K. M., & Fiala, J. C. (2002). Endosomal compartments serve multiple hippocampal dendritic spines from a widespread rather than a local store of recycling membrane. *Journal on Neuroscience, 22*, 2215–2224.
Cottrell, J. R., Dube, G. R., Egles, C., & Liu, G. (2000). Distribution, density, and clustering of functional glutamate receptors before and after synaptogenesis in hippocampal neurons. *Journal on Neurophysiology, 84*, 1573–1587.
Davis, G. (2006). Homeostatic control of neural activity: From phenomenology to molecular design. *Annual Review of Neuroscience, 29*, 307–323.
Derkach, V. A., Oh, M. C., Guire, E. S., & Soderling, T. R. (2007). Regulatory mechanism of AMPA receptors in synaptic plasticity. *Nature Reviews. Neuroscience, 8*, 101–113.
Dudek, S. M., & Bear, M. F. (1992). Homosynaptic long-term depression in area CA1 of hippocampus and effects of *N*-methyl-D-aspartate receptor blockade. *Proceedings of the National Academy of Sciences of the United States of America, 89*, 4363–4367.
Dudek, S. M., & Bear, M. F. (1993). Bidirectional long-term modification of synaptic effectiveness in the adult and immature hippocampus. *Journal on Neuroscience, 13*, 2910–2918.
Earnshaw, B. A., & Bressloff, P. C. (2006). A biophysical model of AMPA receptor trafficking and its regulation during LTP/LTD. *Journal on Neuroscience, 26*, 12362–12367.
Ehlers, M. D. (2000). Reinsertion or degradation of AMPA receptors determined by activity-dependent endocytic sorting. *Neuron, 28*, 511–525.
Ehlers, M. D. (2003). Activity level controls postsynaptic composition and signaling via the ubiquitin-proteasome system. *Nature Neuroscience, 6*, 231–242.
Groc, L., Heine, M., Cognet, L., Brickley, K., Stephenson, F. A., Lounis, B., et al. (2004). Differential activity-dependent regulation of the lateral mobilities of AMPA and NMDA receptors. *Nature Neuroscience, 7*, 695–696.
Hausser, M. (2001). Synaptic function: Dendritic democracy. *Current Biology, 11*, R10–R12.
Hayer, A., & Bhalla, U. S. (2005). Molecular switches at the synapse emerge from receptor and kinase traffic. *PLoS Computers in Biology, 1*, 137–154.
Holcman, D., & Schuss, Z. (2004). Escape through a small opening: receptor trafficking in a synaptic membrane. *Journal of Statistical Physics, 117*, 976–1014.
Holcman, D., & Triller, A. (2006). Modeling synaptic dynamics driven by receptor lateral diffusion. *Biophysical Journal, 91*, 2405–2415.
Holmes, W. R., & Grover, L. M. (2006). Quantifying the magnitude of changes in synaptic levels parameters with long-term potentiation. *Journal on Neurophysiology, 96*, 1478–1491.
Ju, W., Morishita, W., Tsui, J., Gaietta, G., Deerinck, T. J., Adams, S. R., et al. (2004). Activity-dependent regulation of dendritic synthesis and trafficking of AMPA receptors. *Nature Neuroscience, 7*, 244–253.
Kelleher, R. J., Govindarajan, A., & Tonegawa, S. (2004). Translational regulatory mechanisms in persistent forms of synaptic plasticity. *Neuron, 44*, 59–73.
Kennedy, M. J., & Ehlers, M. (2006). Organelles and trafficking machinery for postsynaptic plasticity. *Annual Review Neuroscience, 29*, 325–362.
Kim, C. H., & Lisman, J. E. (2001). A labile component of AMPA receptor-mediated synaptic transmission is dependent on microtubule motors, actin, and *N*-ethylmaleimide-sensitive factor. *Journal on Neuroscience, 21*, 4188–4194.
Koch, C. (1999). *Biophysics of computation*. Oxford University Press.
Konur, S., Rabinowitz, D., Fenstermaker, V. L., & Yuste, R. (2003). Regulation of spine sizes and densities in pyramidal neurons. *Journal on Neurobiology, 56*, 95–112.
Lamprecht, R., & LeDoux, J. (2004). Structural plasticity and memory. *Nature Reviews. Neuroscience, 5*, 45–54.
Lauffenberger, D. A., & Linderman, J. J. (1993). *Receptors: Models for binding, trafficking and signaling*. New York: Oxford University Press.
Lin, J. W., Ju, W., Foster, K., Lee, S. H., Ahmadian, G., Wyszynski, M., et al. (2000). Distinct molecular mechanisms and divergent endocytotic pathways of AMPA receptor internalization. *Nature Neuroscience, 3*, 1282–1290.
Luscher, C., Xia, H., Beattie, E. C., Carroll, R. C., von Zastrow, M., Malenka, R. C., et al. (1999). Role of AMPA receptor cycling in synaptic transmission and plasticity. *Neuron, 24*, 649–658.
Magee, J. C., & Cook, E. P. (2000). Somatic EPSP amplitude is independent of synapse location in hippocampal pyramidal neurons. *Nature Neuroscience, 3*, 895–903.
Malenka, R. C., & Bear, M. F. (2004). LTP and LTD: An embarrassment of riches. *Neuron, 44*, 5–21.
Malinow, R., & Malenka, R. C. (2002). AMPA receptor trafficking and synaptic plasticity. *Annual Review of Neuroscience, 25*, 103–126.
Matsuzaki, M., Honkura, N., Ellis-Davies, G. C. R., & Kasai, H. (2004). Structural basis of long-term potentiation in single dendritic spines. *Nature, 429*, 761–766.
McCormack, S. G., Stornetta, R. L., & Zhu, J. J. (2006). Synaptic AMPA receptor exchange maintains bidirectional plasticity. *Neuron, 50*, 75–88.
Nimchinsky, E. A., Sabatini, B. L., & Svoboda, K. (2002). Structure and function of dendritic spines. *Annual Review Physiology, 64*, 313–353.
Nusser, Z., Lujan, R., Laube, L., Roberts, J. D. B., Molnar, E., & Somogyi, P. (1998). Cell type and pathway dependence of synaptic AMPA receptor number and variability in the hippocampus. *Neuron, 21*, 545–549.
O'Brien, R. J., Kamboj, S., Ehlers, M. D., Rosen, K. R., Fischbach, G. D., & Huganir, R. L. (1998). Activity-dependent modulation of synaptic AMPA receptor accumulation. *Neuron, 21*, 1067–1078.
Palmer, C. L., Cotton, L., & Henley, J. M. (2005). The molecular pharmacology and cell biology of alpha-amino-3-hydroxy-5-methyl-4-isoxazolepropionic acid receptors. *Pharmacological Reviews, 57*, 253–277.
Passafaro, M., Piech, V., & Sheng, M. (2001). Subunit-specific temporal and spatial patterns of AMPA receptor exocytosis in hippocampal neurons. *Nature Neuroscience, 4*, 917–926.
Piccini, A., & Malinow, P. (2002). Critical postsynaptic density 95/disc large/zonula occludens-1 interactions by glutamate receptor 1 (GluR1) and GluR2 required at different subcellular sites. *Journal of Neuroscience, 22*, 5387–5392.
Pierce, J. P., van Leyen, K., & McCarthy, J. B. (2000). Translocation machinery for synthesis of integral membrane and

secretory proteins in dendritic spines. *Nature Neuroscience, 3*, 311–313.

Rall, W. (1962). Theory of Physiological properties of dendrites. *Annals of the New York Academy of Sciences, 96*, 1071–1092.

Rumsey, C. C., & Abbott, L. F. (2006). Synaptic democracy in active dendrites. *Journal of Neurophysilogy, 96*, 2307–2318.

Sekine-Aizawa, Y., & Huganir, R. L. (2004). Imaging of receptor trafficking by using α-bungarotoxin-binding-site-tagged receptors. *Proceedings of the National Academy of Sciences, 101*, 17114–17119.

Setou, M., Seog, D. H., Tanaka, Y., Kanai, Y., Takei, Y., et al. (2002). Glutamate-receptor-interacting protein GRIP1 directly steers kinesin to dendrites. *Nature*, 417, 83–87.

Sheng, M., & Kim, M. J. (2002). Postsynaptic signaling and plasticity mechanisms. *Science, 298*, 776–780.

Shi, S., Hayashi, Y., Esteban, J. A., & Malinow, R. (2001). Subunit-specific rules governing AMPA receptor trafficking to synapses in hippocampal pyramidal neurons. *Cell, 105*, 331–343.

Shouval, H. Z., Bear, M. F., & Cooper, L. N. (2002a). A unified model of NMDA receptordependent bidirectional synaptic plasticity. *Proceedings of the National Academy of Sciences of the United States of America, 99*, 10831–10836.

Shouval, H. Z., Castellani, G. C., Blais, B. S., Yeung, L. C., & Cooper, L. N. (2002b). Converging evidence for a simplified biophysical model of synaptic plasticity. *Biological Cybernetics, 87*, 383–391.

Shouval, H. Z. (2005). Clusters of interacting receptors can stabilize synaptic efficacies. *Proceedings of the National Academy of Sciences of the United States of America, 102*, 14440–14445.

Sorra, K. E., & Harris, K. M. (2000). Overview on the structure, composition, function, development, and plasticity of hippocampal dendritic spines. *Hippocampus, 10*, 501–511.

Song, I., & Huganir, R. L. (2002). Regulation of AMPA receptors during synaptic plasticity. *Trends in Neurosciences, 25*, 578–588.

Sutton, M. A., & Schuman, E. M. (2005). Local translational control in dendrites and its role in long-term synaptic plasticity. *Journal on Neurobiology, 64*, 116–131.

Tanaka, J.-I., Matsuzaki, M., Tarusawa, E., Momiyama, A., Molnar, E., Kasai, H., et al. (2005). Number and density of AMPA receptors in single synapses in immature cerebellum. *Journal on Neuroscience, 25*, 799–807.

Tardin, C., Cognet, L., Bats, C., Lounis, B., & Choquet, D. (2003). Direct imaging of lateral movements of AMPA receptors inside synapses. *EMBO Journal, 22*, 4656–4665.

Triller, A., & Choquet, D. (2003). Synaptic structure and diffusion dynamics of synaptic receptors. *Biology of the Cell, 95*, 465–476.

Triller, A., & Choquet, D. (2005). Surface trafficking of receptors between synaptic and extrasynaptic membranes. *Trends in Neurosciences, 28*, 133–139.

Tuckwell, H. C. (1988). *Introduction to theoretical neurobiology*. New York: Cambridge University Press.

Turrigiano, G. G., Leslie, K. R., Desai, N. S., Rutherford, L. C., & Nelson, S. B. (1998). Activity-dependent scaling of quantal amplitude in neocortical neurons. *Nature, 391*, 892–895.

Turrigiano, G. G., & Nelson, S. B. (2004). Homeostatic plasticity in the developing nervous system. *Nature Reviews. Neuroscience, 5*, 97–107.

Van Kampen, N. G. (1992). *Stochastic processes in physics and chemistry*. North-Holland, Amsterdam.

Zhabotinsky, A. M., Camp, R. N., Epstein, I. R., & Lisman, J. E. (2006). Role of neurogranin concentrated in spines in the induction of long-term potentiation. *Journal on Neuroscience, 26*, 7337–7347.